Answer to Reviewer 1

In this study, the authors present a new open-access web-based platform with visualization and easy-access to simulations with the lake model Simstrat v2.1 for 54 lakes in Switzerland. The practical use of the platform is illustrated with two case studies, one to assess the effects of past climate change on the thermal structure of a lake, and second how short extreme events temporally affect the lake thermal structure. The presented platform is state-of-the-art but this might be stressed in the paper even more. Furthermore, the manuscript could benefit from some structural and textual changes, of which I included a list with suggestions under 'textual comments'. In general, the study can only be considered for publication if the comments specified here below are sufficiently addressed

We thank Reviewer 1 for his comments. We agree to stress more that the web-based one-dimensional hydrodynamic platform is state-of-the-art. This is now better stressed in the abstract, the introduction and the conclusion. We have also applied the structural and editing changes requested and thank the reviewer for this and took the opportunity of this review to extensively rework the manuscript.

General Comments

1. The main topic of the paper is to present the new online platform: I think this could be promoted even more throughout the paper:

a. The last paragraph of the introduction could be more elaborated. Also rewrite the sentence with 'with the intention of making our results openly accessible'. From what I understand, they are already open. More details could be provided on what is present on the platform. (In the introduction and/or in the results section, (P5 L13-15).

We have rewritten the last paragraph of the introduction. It now reads: "In this work, we present a new automated web-based platform to visualize and distribute the near real time (weakly) output of the one-dimensional hydrodynamic lake model Simstrat through an user-friendly web interface. The current version includes 54 Swiss lakes covering a wide range of characteristics from very small volume such as Inkwilersee (9 x 10^{-3} km^3) to very large systems such as Lake Geneva (89 km^3), over an altitudinal gradient (Lago Maggiore at from 193 m. a.s.l. to Daubensee at 2207 m. a.s.l.) and over all trophic states (14 euthrophic lakes, 10 mesotrophic lakes and 21 oligotrophic lakes, Appendix A). We focus here on describing the fully automated workflow, which simulates the thermal structure of the lakes and weekly updates the online platform (https://simstrat.eawag.ch) with metadata, plots and downloadable results. This state-of-the-art framework is not restricted to the currently selected lakes and can be applied to other systems or at global scale."

We have restructured the section 2.4 and the last paragraph was extended and moved to the beginning of the section. We also now provide more details on what is present on the platform

b. In the conclusion the main results of the two case studies as main advantages of the platform should be highlighted. I would also end the conclusion with a general statement about the platform.

We have modified the conclusion to better reflect the results from the case studies: "We demonstrated the benefit of the platform through two simple case studies. First, we showed that the high frequency modelled temperature data allows a complete assessment of the effect of climate change on the thermal structure of a lake. We specifically show the need to evaluate changes in all atmospheric forcing, in the watershed or through-flow heat energy and in light penetration to accurately assess the evolution of the lake thermal structure. Then we showed that the high frequency modelled data can be used to investigate special events such as wind storms, there in-situ measurements under current temporal resolution are failing. ".

We have also added a more general statement regarding the platform at the end of the conclusion with the following sentences "By promoting a cross-exchange of expertise through openly sharing of in-situ and model data at high frequency, this open-access data platform is a new path forward for scientists and practitioners. "

2. The manuscript could benefit from a slightly adjusted structure. Now, the results sections 3.1 and 3.2 describing the two case studies also include methodology and even literature review parts. Therefore I suggest to use a new structure as follows:

2. Methods

2.5. Case Studies

2.5.1. Long-term evolution of the thermal structure of lakes: Lake Biel Insert here paragraph 1 of page 6

2.5.2. Event based evolution of the lake thermal structure Add here first paragraph of page 7

We agreed that the case studies should be introduced in the method section. We have added a subsection 2.5 Case studies where we briefly present the 2 case studies.

Specific comments

1. In the abstract, it would be good to specify that the lakes on the platform are modeled with one lake model, Simstrat. Also the sentences could be rephrased more directly. Some examples are included in the textual comments.
   The model is indicated in the title and as website. We do not think it is necessary to repeat the information.

2. P3 L19: ‘an online platform’: be more specific on which online platform: the new platform you present in this study? (see also general comment)
   Changed to” update the simstrat.eawag.ch online data platform to display”

3. Figure 1: Please make the titles of the input and output boxes consistent. I suggest to only use ‘input’ and ‘output’ (so remove the ‘data’ in ‘input data’). Please apply the same consistency in the figure legend and caption.
   We have modified the figure and the caption accordingly

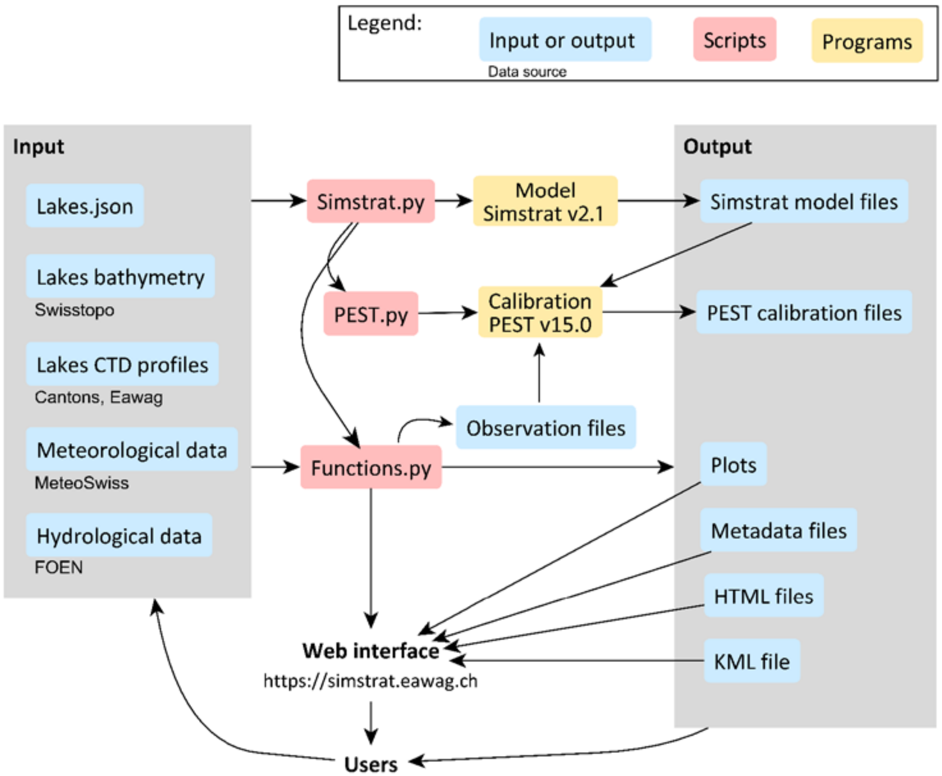

Figure 1. General workflow diagram. Model input (left box) is retrieved and processed by the Python script "Simstrat.py", which runs the model (Simstrat v2.1) and/or model calibration (using PEST v15.0) and produces output (right box). This output is then uploaded to a web interface (https://simstrat.eawag.ch) for general use. All scripts and programs are available on https://github.com/Eawag-AppliedSystemAnalysis/Simstrat/releases/tag/v2.1 and https://github.com/Eawag-AppliedSystemAnalysis/Simstrat-WorkflowModellingSwissLakes. Simstrat = one dimensional hydrodynamic model; CTD = Conductivity, Temperature, Depth profiler; PEST = Model independent parameter estimation and uncertainty analysis software; FOEN = Swiss Federal Office of Environment; MeteoSwiss = Swiss Federal Office of Meteorology and Climatology; Swisstopo = Swiss Federal Office of Topography

4. Figure 2: Please add color bar of lake temperatures and scale bar to figure. What is the green color on the figure representing? Please also add this in figure or figure caption.
   We now use the same color for each lake. The legend of the map is indicated as a link in the caption.

   We also now have indicated the locations of the 54 lakes.

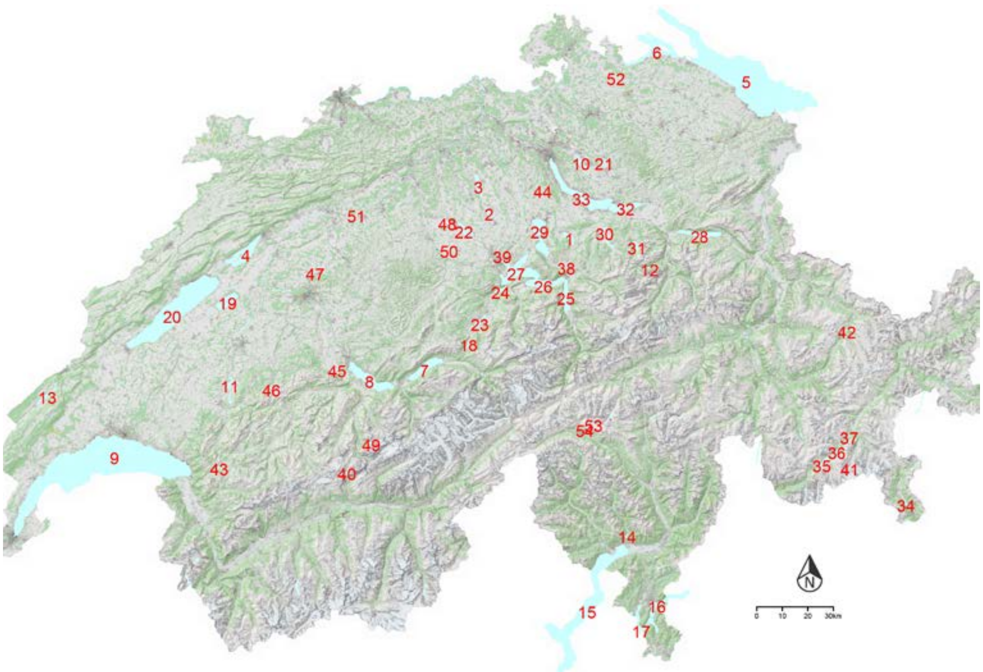

Figure 2. Illustration of the interactive map displayed on the homepage of the online platform: https://simstrat.eawag.ch. The location of the lakes discussed in this manuscript is also indicated with numbers (See Appendix A). Basemap is provided by Swisstopo and the specific legend can be found here https://api3.geo.admin.ch/static/images/legends/ch.swisstopo.swisstlm3d-karte-farbe_en_big.pdf

5. The authors state that 'inflows are disabled if no discharge or temperature data is available' (P4, L1). Is this the case for many lakes? Please identify the relevant lakes in Appendix table A and add

the number in the text. Please also include a statement on the sensitivity of this methodological choice.

We have modified the Appendix A to better indicate this. We also added the theoretical residence time when data are available. In all low altitude lakes, lakes where the discharge is not accounted for are lakes with very weak inflows/outflows and large retention time. The influence on the thermal structure is therefore minimal. The problem is potentially larger for small high altitude lakes and should be further investigated in the future. Missing inflows and more generally watershed data is a source of error in small alpine lakes, yet, such error can be compensated during the calibration process. We have modified the text accordingly: "The aggregated discharge is the sum of the discharge of all inflows, and the aggregated temperature is the weighted average of the inflows for which temperature is measured. Inflow data are often missing for small or high altitude lakes (Appendix A). Missing inflows and more generally watershed data is a source of error in small alpine lakes, yet, such error can be compensated during the calibration process."

6. P4 L2-5 and Appendix table A: please also indicate in the table for which lakes the Secchi depth measurements are available. Please also add a column with the lake tropic status, or provide the methodology of the classification in this paragraph.

   We have added a new column regarding the trophic state and explicitly indicated the lakes with observed secchi depth information

7. For the story continuation it is better to switch the third and second paragraph of P4. Like this, it makes more sense to first describe the timeframes and then how data gaps are treated. Please also take care of the transition in the data-gap paragraph.

   We have reversed and then merged and finally slightly extended the paragraph:

"The timeframe of the model is determined by the availability of the meteorological data (air temperature, solar radiation, humidity, wind, precipitation). Initial conditions for temperature and salinity are set using conductivity-temperature-depth (CTD) profiles or using the temperature information from the closest lake. We apply different data patching methods to remove data gaps from the forcing depending on the length of the data gap. For small data gaps with duration not exceeding one day, the dataset is linearly interpolated. In total < 1 % of the dataset is corrected using this approach. Longer data gaps of up to 20 days are replaced by the long-term average values for the corresponding day of the year. Only ~ 1.5 % of the dataset is corrected using this approach”

8. P4 L13-14: It is not clear to where the observations from the CTD profiles comes from. Please add the data source.
All the data source are provided as a link to the online platform in the acknowledgment

9. P4 L17: please add more details on how the parameters for calibration were selected, at least include a reference of the previous sensitivity analysis.
We added the following text to the Calibration section
“Model parameters are set to standard default values, and four of them are calibrated (see Table 2). The parameters p_radin and and f_wind scale the incoming long-wave radiation and the wind speed, respectively, and can be used to compensate for systematic differences between the meteorological conditions on the lake and at the closest meteo station. The parameter a_seiche determines the fraction of wind energy that feeds the internal seiches. This parameter is lake-specific, as it depends on the lake’s morphology and it's exposition to different wind directions. Finally, the parameter p_albedo scales the albedo of ice and snow applied to incoming shortwave radiation, which depends on the ice/snow cover properties and is unknown for the individual lakes. The calibration parameters were selected according to their importance for the model (e.g. based on previous sensitivity analysis), and their number was deliberately kept small in order to keep the calibration process simple and focused. Calibration is performed using PEST v15.0 (see http://pesthomepage.org), a model-independent parameter estimation software (Doherty, 2016).”

10. P4 L21: ‘unless significant changes are made to either the model, forcing data or observational data’. In when is this the case? Please add more textual details on this.
We added the following information to the text: “e.g. release of a new version of Simstrat or delivery of a large amount of new observational data”

11. P4 L26: Please add the source of lake volume, temperature and densities.
Lake volume are extracted from Swisstopo the Swiss Federal Office of Topography,

In situ observations comes from cantonal agencies or organisation such CIPEL (for Lake Geneva). They are indicated in the acknowledgment and fully listed on the web-based platform

12. P5 L25-27: I would elaborate this paragraph, and discuss also the correlation coefficient showed in figure 3. Please also list the six lakes not shown in the figure caption.
    The six lakes with too large RMSE are now indicated with the symbol "°" in Figure 3.

    We also discussed slightly more the model performance shown on Figure 3:
    "The correlation coefficient remains always higher than 0.93 suggesting also that the model successfully reproduce the thermal structure of the investigated lakes. Overall, the quality of the results is better for lowland lakes than for high altitude lakes where local meteorological and watershed information are often missing."

13. P5 L27: Please add more info to the study of Bruce et al., 2018: is it a global lake modelling study? Do they incorporate lakes in Switzerland as well?
    We have modified the text and added the following information: "This is comparable to the RMSE range of ~0.7-2.1 °C reported in a recent global 32-lake modelling study using GLM (Bruce et al., 2018) also including Lake Geneva, Lake Constance and Lake Zurich."

14. P6 L26-31: On line 26 there is indicated that a 'similar analysis' is done for all modelled lakes, however, only an inter-comparison of winter and summer stratification is showed and discussed, while in the case study for Lake Brienz, the trends in stratifications are investigated. Please rewrite the text to be consistent with the figures showed. Please add also more information on the possible implications of the delay of melt water runoff. Also, in the caption figure 6, there is no information on winter stratification, but on ice cover. Please update the text so that it is consistent with the information on the figure.
    We agree with the Reviewer that we actually do not show the same analysis for all modelled lakes. This analysis cannot be summarized in 1 page in this manuscript and we have reformulated this statement accordingly. We also have modified the text regarding ice coverage and not inverse stratification as previously written. Note also that Figure 6 is now Figure 5. We removed the previous Figure 5 that was not necessary for this manuscript. The modified text related to this change is:

"Such analyses can be extended to all modelled lakes. An inter-comparison of the temporal extent of summer stratification and winter ice cover period is illustrated in Figure 5."

15. Figure 7: Please remove X and Y labels, and add 'in Schmidt stability' to 'Delay/ Recovery time' colorbar caption.
    Modified

Answer to Reviewer 2

General comments:

Gaudard et al. presents a web-based platform for visualization and promotion of lake model outputs that are openly accessible to the general public. The web-based platform currently includes 54 lakes in Switzerland, and it could be useful in synthesizing lake model outputs in other geographical regions.

We thank Reviewer 2 for his comments

Specific comments:

Pg1, L13-14: and appropriate model, unless the authors have validated Simstrat v2.1

Simstrat v2.1 is validated for mid latitudes lakes and previous version were used in tropical lakes. We believe that this model can be used at global scale

Pg2, L24: please replace ‘It’ with a real subject (e.g., model output data) to avoid potential interpretation confusion for this sentence.

The sentence has been modified:

“Yet, model output data should not only be seen as a tool for temporal interpolation of measurements. Models also provide data of hard to measure quantities which are helpful for specific analyses (e.g., the heat content change to assess impact of climate change, or the vertical diffusivity to estimate vertical turbulent transport). Models finally support the interpretation of biogeochemical processes which often depend on the thermal stratification, mixing and temperature”

Pg2, L26-27: ‘and it can support the interpretation of biogeochemical observations, if the relevant processes are driven by thermal stratification and mixing’. This is confusing- does it mean models cannot support the interpretation of biogeochemical observations if the relevant processes are NOT driven by thermal stratification and mixing?

Our model is a physical model for temperature, stratification and mixing in lakes. It is therefore correct that it can only help interpreting biogeochemical processes, if they are influenced by the physical processes. However, most biogeochemical processes in lakes are to some extent influenced by stratification, mixing and/or temperature. To clarify this, we modified the sentence to:

"Models finally support the interpretation of biogeochemical processes which often depend on the thermal stratification, mixing and temperature".

Pg3, L26-27: please replace 'adiabatic vertical rate' with the commonly used 'adiabatic lapse rate'. What are the ranges of altitude difference between the lakes and the meteorological stations? Adiabatic lapse rate is not necessarily -6.5 C/km, so such assumption could result significant errors when the altitude difference is large.

We have modified the sentence and have added a table indicating the altitude and coordinate of all meteorological stations used in this study. The difference is typically O(10m) for low land lakes but this difference is indeed large for high alpine lakes like Lake Ritom and Lake Cadagno (~1000 m of altitude difference compared to the meteorological station), Daubensee (~ 800 m of altitude difference). We now indicate in the manuscript that meteorological station near high altitude lakes would be needed. "This correction is a source of error in high altitude lakes like Daubensee for which dedicated meteorological station would be needed."

Pg4, L3-5: any reference that supports the light absorption coefficient parameterization described here?

We refrain to refer to all papers providing secchi disk information on a Swiss lake. We used one already cited reference (Schwefel et al. 2016)

Pg4, L8-10: what's the gap size for the 'highly seasonal variables'? How large is the inter annual variability for the 'highly seasonal variables', based on available measurements?

We have rewritten the paragraph as follow: "The timeframe of the model is determined by the availability of the meteorological data (air temperature, solar radiation, humidity, wind, precipitation). Initial conditions for temperature and salinity are set using conductivity-temperature-depth (CTD) profiles or using the temperature information from the closest lake. We apply different data patching methods to remove data gaps from the forcing depending on the length of the data gap. For small data gaps with duration not exceeding one day, the dataset is linearly interpolated. In total < 1 % of the dataset is corrected using this approach. Longer data gaps of up to 20 days are replaced by the long-term average values for the corresponding day of the year. Only ~ 1.5 % of the dataset is corrected using this approach."

Pg5, L7: how do the authors determine the existence of ice? Is it measured or modeled?

The existence of ice is modeled. The model presented in Appendix B has been calibrated for Swiss lakes based on in situ observation of ice cover.

Pg5, L25: what is the model validation period for RMSE? Is it the model timeframe listed in appendix A?

Indeed. We have decided to use the entire time series and do not split between a calibration and a validation period. This could be done for the lakes having long time series of observations but reduce the accuracy of the calibrated parameters for shorter time series of observations

Pg 5, L 26: how large were the overestimations in the 6 lakes with RMSE > 2C?

We have modified the sentence as follow: "Out of the 46 calibrated lakes, the post-calibration root mean square error (RMSE) is < 1 °C for 17 lakes, between 1 and 1.5 °C for 15 lakes, between 1.5 and 2 °C for 8 lakes and between 2 °C and 3°C for 6 lakes (Figure 3), calibration data was not sufficient for 8 lakes in which we used standard settings."

Pg 6, L9: is the 'surface temperature' air temperature at the surface or lake surface temperature? Could the authors plot measured air temperature in Figure 4a?

We thank the reviewer for this comment that helped to rethink the Figure 4. We now also indicated other temperatures such as air temperature, total lake temperature and tributaries temperature. We show that the lake surface temperature (not the entire lake) is warming at a faster rate than the air temperature and discuss this in section 3.1.

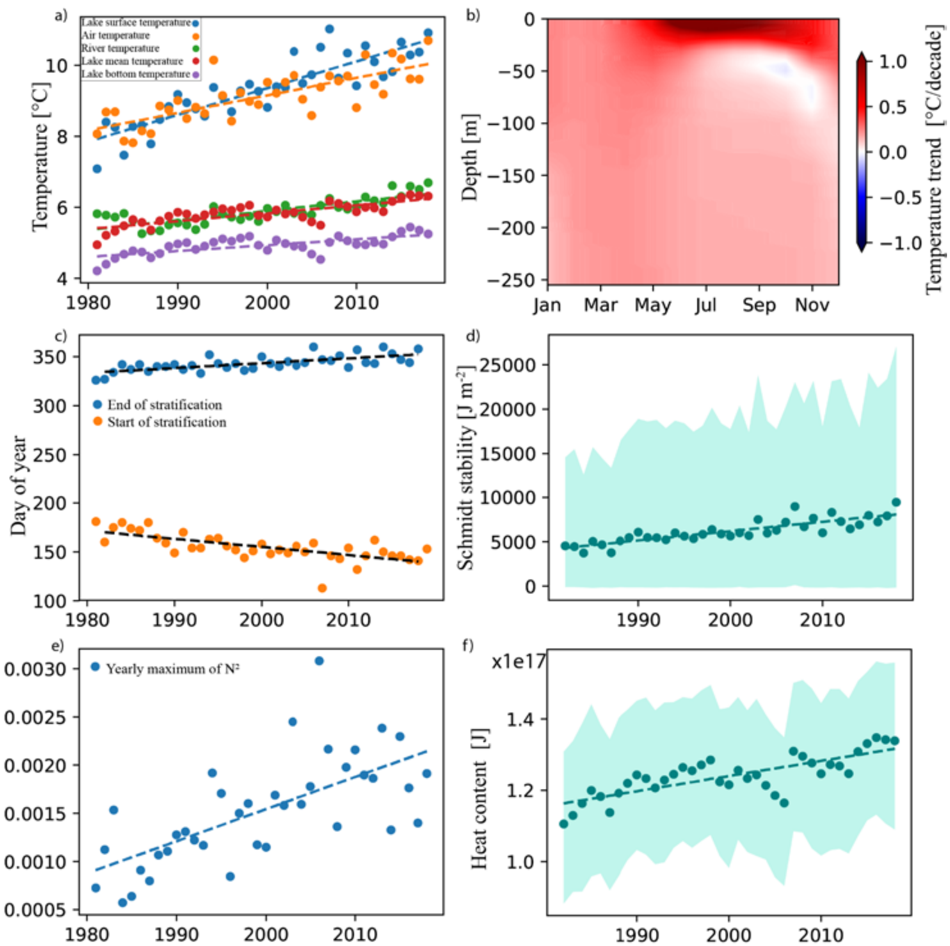

Figure 4. Evolution of several indicators for Lake Brienz over the period 1981-2018; all linear regression have p_values << 0.001: (a) yearly mean lake surface temperature (0.74 °C/decade), yearly mean air temperatures (0.50 °C/decade), yearly mean tributary temperatures (0.26 °C/decade), yearly mean lake temperatures (0.22 °C/decade) and yearly mean bottom temperatures (0.16 °C/decade), with linear regression, (b) contour plot of the linear temperature trend through depth and month, (c) yearly start (+3.7 days/decade) and end (-7.5 days/decade) day of summer stratification, with linear regression, (d) yearly mean (line), min and max (shaded area) Schmidt stability, with linear regression, (e) yearly maximum Brunt-Väisälä frequency (3.3×10^{-4} $1/s^2$/decade), with linear regression (f) yearly mean (line), min and max (shaded area) heat content.

Pg 6, L20: Figures 4e and 4e

Modified

Discussion paper P12, Fig1: please provide the full names of each abbreviation, e.g., what are Swisstopo, CTD, FOEN? Some abbreviations are defined in the main text (but scattering around), and it would be very helpful to list them in the figure caption. Also, observation files should be listed as an intermedium product instead of an output.

We have modified Figure 1 as well as the caption

Answer to Reviewer 3

General Comments

In this paper the authors describe the development of an openly accessible web-based platform for visualization and data access of 54 lakes modelling in Switzerland. The lake modelling is conducted with a one-dimensional lake model Simstrat v2.1, which is the core scientific component of this paper. The other important component of this paper is the lake modelling platform, which is beneficial to both the general public and researchers. It is good that both components are included in this study; nevertheless, both components are not thoroughly introduced. As a scientific publication, higher portion of new scientific modules in Simstrat v2.1 and using Simstrat v2.1 for the scientific findings in a single event or from long-term climatic trends can benefit this paper.

We thank Reviewer 3 for his/her comments. We have largely reworked the manuscript to better show how the web-based platform can be used for scientific purpose. This is mostly evident in the section 3.1

Specific Comments

1. The drawback of one-dimensional lake model is the lack of water circulation; nevertheless, the thermal dynamic in the lake can be very different from small lake to large one. Surface of the 54 studied lakes ranges from 0.102-km2 of Lake Inkwilersee to 580-km2 of Lake Geneva, which are quite diverse in horizontal dimension. It is not mentioned in the paper about the limitations and differences of applying one-dimensional Simstrat v2.1 to small and large lakes.

The main limitation of 1D vertical model is that spatial variability is not accounted for. This is the reason why multibasin lakes like Lake Lucerne have been split into 4 different lakes characterised by distinct basin. This is the same for Lake Zurich, Lake Constance and Lake Lugano. We have written the following in the document: "For lakes with clearly defined multi basin such as Lake Lucerne, Lake Zurich, Lake Constance and Lake Lugano, each basin is considered as a separated lake connected to the other basins by inflows/outflows "

2. In this study, four parameters among 46 lakes were calibrated. Now only the temperatures of post-calibration root mean square error were described. It would be good to summarize the calibrating

processes, and the physical meanings of the calibrated parameters and its relationship to lake area and lake characters.

We have added the following text:

"Model parameters are set to standard default values, and four of them are calibrated (see Table 2). The parameters *p_radin* and and *f_wind* scale the incoming long-wave radiation and the wind speed, respectively, and can be used to compensate for systematic differences between the meteorological conditions on the lake and at the closest meteo station. The parameter *a_seiche* determines the fraction of wind energy that feeds the internal seiches. This parameter is lake-specific, as it depends on the lake's morphology and it's exposition to different wind directions. Finally, the parameter *p_albedo* scales the albedo of ice and snow applied to incoming shortwave radiation, which depends on the ice/snow cover properties and is unknown for the individual lakes. The calibration parameters were selected according to their importance for the model (e.g. based on previous sensitivity analysis), and their number was deliberately kept small in order to keep the calibration process simple and focused. Calibration is performed using PEST v15.0 (see http://pesthomepage.org), a model-independent parameter estimation software (Doherty, 2016)"

3. P4, L1~5: In this study, the light absorption coefficient plays an important role determining incoming heat flux. Is there any reference, except current cited one (Poole and Atkins, 1929), using similar parameterization?

The parameterization of the light absorption using a beer lamber law parameterized by one coefficient is the standard for limnological study. We added a more recent references (already used in the manuscript) to highlight this

4. P4, L6: What is the percentage of the missing forcing data in this study? And what is the impact of discrepancy in the model?

We have modified the text as follow:

"The timeframe of the model is determined by the availability of the meteorological data (air temperature, solar radiation, humidity, wind, precipitation). Initial conditions for temperature and salinity are set using conductivity-temperature-depth (CTD) profiles or using the temperature information from the closest lake. We apply different data patching methods to remove data gaps from the forcing depending on the length of the data gap. For small data gaps with duration not exceeding one day, the dataset is linearly interpolated. In total < 1 % of the dataset is corrected using this approach. Longer data gaps of up to 20 days are replaced by the long-term average values for the corresponding day of the year. Only ~ 1.5 % of the dataset is corrected using this approach"

5. P4, L10~11: It is not clear how the variable "cloud coverage" is used in the model, as the measured solar radiation is available.

Cloud coverage is needed for estimating incoming long wave radiation while solar radiation are needed for short wave radiation.

6. P4, L13~14: Are all the lakes initialized for temperature and salinity using CTD profiles?

Most lakes are initialized with data from CTD profiles. When not available, use information from the closest lake. The small discrepancy with the real temperature profile is quickly reduced (after < 6 months). The text was modified to better indicate this

7. P5, L13: Why the platform is automatically updated with a weekly frequency?

We did not think it was necessary to update it more frequently but already got multiple request to reduce the update frequency to the day. There is no technical obstacle but we prefer to work in improving the pipeline first.

Textual Comments

1. P4, L27: Missing a comma "," between the heat capacity of water and the volume of the lake.

modified

Toward an open-access of high-frequency lake modelling and statistics data for scientists and practitioners. The case of Swiss Lakes using Simstrat v2.1

Adrien Gaudard[1†], Love Råman Vinnå[1], Fabian Bärenbold[1], Martin Schmid[1], Damien Bouffard[1]

[1]Surface Waters Research and Management, Eawag, Swiss Federal Institute of Aquatic Sciences and Technology, Kastanienbaum, Switzerland

[†] deceased, 2019

Correspondence to: Damien Bouffard (damien.bouffard@eawag.ch)

Abstract

One-dimensional hydrodynamic ~~lake~~ models are nowadays widely recognized as key tools~~.~~ for lake studies. They offer the possibility to ~~study~~analyse processes at high frequency, here referring to hourly time scale, to ~~analyse~~investigate scenarios and test ~~hypothesizes~~hypotheses. Yet, simulation outputs are mainly used by the modellers themselves and often not easily reachable for the outside community. We have developed an ~~openly accessible~~open-access web-based platform for visualization and promotion of easy access to lake model output data updated in near real time (simstrat.eawag.ch). This platform was developed for 54 lakes in Switzerland with potential for adaptation to other ~~regional areas~~regions or ~~even~~ at global ~~worldwide~~ scale using appropriate forcing input data. The benefit of this data platform is ~~here~~ practically illustrated with two examples. First, we show that the output data allows for assessing the long term effects of past climate change on the thermal structure of a lake. ~~In the second case, we demonstrate~~The study confirms the need to not only evaluate changes in all atmospheric forcing but also changes in the watershed or through-flow heat energy and changes in light penetration to assess the lake thermal structure. Then, we show how the data platform can be used to study and compare the role of episodic strong wind events for different lakes on a regional scale and especially how ~~they temporary destabilize~~ their thermal structure~~.~~ is temporarily destabilized. With this open~~-~~-access data platform we demonstrate ~~the~~a new path forward for scientists and practitioners promoting a cross-exchange of expertise through openly sharing of in-situ and model data.

1 Introduction

Aquatic research is particularly oriented towards providing relevant tools and expertise for practitioners. Understanding and monitoring inland waters is ~~most~~ often based on *in situ* observations. Today, the physical and biogeochemical properties of many lakes are monitored using monthly to bi-monthly vertical discrete profiles. Yet, part of the dynamics is not captured at this temporal scale (Kiefer et al., 2015). An emerging alternative approach consists in deploying long-term moorings with sensors and loggers at different depths of the water column. However, this approach is ~~scarcely~~seldom used for country-level monitoring~~ purposes at the country scale~~, although it is promoted by research initiatives such as GLEON (Hamilton et al., 2015) or NETLAKE (Jennings et al., 2017).

It is common to parameterize aquatic physical processes with mechanistic models, and ultimately use them to understand aquatic systems through scenario investigation or ~~climate~~ projection~~.~~ of trends in for example a climate setting. In the last decades, many lake models have been developed. ~~Although never perfect, they have been shown to~~They often successfully reproduce~~ very well~~ the thermal structure of natural lakes (Bruce et al., 2018). Today's most widely referenced one-dimensional (1D) models include (alphabetic order) DYRESM (Antenucci and Imerito, 2000), FLake (Mironov, 2005), GLM (Hipsey et al., 2014), GOTM (Burchard et al., 1999), LAKE (Stepanenko et al., 2016), Minlake (Riley and Stefan, 1988), MyLake (Saloranta and Andersen, 2007), and Simstrat (Goudsmit et al., 2002). ~~Unfortunately, the~~The results from these models are mainly used by the modellers themselves, and often not easily accessible for the outside community.

The performance of lake models is determined by the physical representativeness of the algorithms and by the quality of the input data. The latter include (i) lake morphology, (ii) atmospheric forcing, (iii) hydrological cycle (e.g. inflow, outflow and/or water level fluctuations), and (iv) light absorption. *In situ* observations~~ (e.g.,~~, such as temperature profiles~~)~~, are ~~often used~~required for calibration of model parameters~~, which remains a time-consuming process. To be successful, such an endeavour requires observations of a broad, representative range of conditions in the system~~. To support this approach, it is important to promote and facilitate the sharing of existing datasets of observations among scientists and practitioners. Conversely, scientists and practitioners should benefit from the model output, which is often ready-to-use, high-frequency and up-to-date. Yet, model output data should not only be seen as a ~~toolbox~~tool for temporal interpolation~~. It~~ of measurements. Models also ~~provides properties that~~provide data of hard to measure quantities which are helpful for specific analyses ~~but difficult to measure~~ (e.g., the heat content change to assess ~~the global~~ impact of climate change, or the vertical diffusivity to estimate vertical turbulent transport~~), and it can~~). Models finally support the interpretation of biogeochemical ~~observations, if the relevant~~ processes ~~are driven by~~ which often depend on the thermal stratification~~ and~~, mixing and temperature. In a global context of open science, collaboration between the different actors and reuse of field and model output data should be fostered. Such win-win collaboration serves the interests of lake modellers, researchers, field scientists, lake managers, lake users, and ~~more generally~~ the public in general.

In this work, we present a new automated web-based platform to visualize and ~~improved version~~ distribute the near real time (weakly) output of the ~~Simstrat~~ one-dimensional hydrodynamic lake model~~. This version is applied as part~~ Simstrat through an user-friendly web interface. The current version includes 54 Swiss lakes covering a wide range of ~~a multi-lake modelling project with the intention of making our extensive results openly accessible.~~characteristics from very small volume such as Inkwilersee (9 x 10^{-3} km^3) to very large systems such as Lake Geneva (89 km^3), over an altitudinal gradient (Lago Maggiore at from 193 m. a.s.l. to Daubensee at 2207 m. a.s.l.) and over all trophic states (14 euthrophic lakes, 10 mesotrophic lakes and 21 oligotrophic lakes, Appendix A). We ~~present~~focus here on describing the ~~deployment of a~~ fully automated workflow, which simulates the thermal structure of the lakes ~~in Switzerland~~ and weekly updates ~~an~~the online platform (https://simstrat.eawag.ch) with metadata, plots and ~~results~~downloadable results. This state-of-the-art framework is not restricted to the currently selected lakes and can be applied to other systems or at global scale.

2 Methods

2.1 Model and workflow

We use the 1D lake model Simstrat v2.1 to model 54 Swiss lakes or ~~basins~~reservoirs (see Appendix A for details of modelled lakes) in an automated way. Simstrat was first introduced by Goudsmit et al. (2002) and has been successfully applied to a number of lakes (Gaudard et al., 2017; Perroud et al., 2009; Råman Vinnå et al., 2018; Schwefel et al., 2016; Thiery et al., 2014). Recently, large parts of the code were refactored using the object-oriented Fortran 2003 standard. This version of Simstrat ~~allows for~~provides a ~~clearer~~clear, modular code structure. The source code of Simstrat v2.1 is ~~openly~~ available via GitHub at: https://github.com/Eawag-AppliedSystemAnalysis/Simstrat/releases/tag/v2.1. ~~In addition to refactoring, a~~A simpler build procedure was implemented using a docker container. This portable build environment contains all necessary software dependencies for the build process of Simstrat. It can ~~thereby~~therefore be used on both Windows and Linux systems. A step-by-step guide is provided on GitHub.

In addition to the improvements already described by Schmid and Köster (2016), Simstrat v2.1 includes (i) the possibility to use gravity-driven inflow and a wind drag coefficient varying with wind speed – both described by Gaudard et al. (2017), and (ii) an ice and snow module. The ice and snow module employed in the model is based on the work of Leppäranta (2014, 2010) and Saloranta and Andersen (2007), and is further described in Appendix B.

A Python script was developed to (i) retrieve the newest forcing data directly from data providers and integrate them into the existing datasets, (ii) process the input data and prepare the full model and calibration setups, (iii) run the calibration of the model for the chosen model parameters, (iv) provide output results, and (v) update ~~an~~the simstrat.eawag.ch online data platform to display these results. The script is controlled by an input file written in JSON format, which specifies the lakes to be modelled together with their physical properties (depth, volume, bathymetry, etc.) and identifies the meteorological and hydrological stations to be used for model forcing. The overall workflow is illustrated in Figure 1.

2.2 Input data

Table 1 summarizes the type and sources of the data fed to Simstrat. For meteorological forcing, homogenized hourly data fromair temperature, wind speed and direction, solar radiation and relative humidity from the Federal Office of Meteorology and Climatology (MeteoSwiss, CH) weather stations are used. For each lake the most relevantclosest weather stations are used. Air temperature is corrected for the small altitude difference (see Appendix A) between the lake and the meteorological station, assuming an adiabatic verticallapse rate of -0.0065 °C m^{-1}. This correction is a source of error in high altitude lakes like Daubensee for which dedicated meteorological station would be needed. The cloud cover needed for downwelling longwave radiations are estimated by comparing observed and theoretical solar radiation (Appendix C). For hydrological forcing, homogenized hourly data from the stations operated by the Federal Office for the Environment (FOEN) are used. For each lake, the data from the available stations at the inflows are aggregated to feed the model with a single inflow. The aggregated discharge is the sum of the discharge of all the inflows, and the aggregated temperature is the weighted average of the inflows for which temperature is measured. Inflows are disabled if no discharge or temperature data is available at all.Inflow data are often missing for small or high altitude lakes (Appendix A). Missing inflows and more generally watershed data is a source of error in small alpine lakes, yet, such error can be compensated during the calibration process. The light absorption coefficient ε_{abs} [m^{-1}] is either obtained from Secchi depth z_{Secchi} [m] measurements, (for Inkwilersee, Lake Biel, Lake Brienz, Lake Geneva, Lake Neuchatel, Lower Lake Zurich, Oeschinensee, Upper Lake Constance, and Sihlsee), or is set to a constant value based on the lake trophic status. In the first case, the following equation is applied: $\varepsilon_{\text{abs}} = 1.7/z_{\text{Secchi}}$ (Poole and Atkins, 1929, Schwefel et al. 2016). In the second case, ε_{abs} is set to 0.15 m^{-1} for oligotrophic lakes, 0.25 m^{-1} for mesotrophic lakes, and 0.50 m^{-1} for eutrophic lakes. The values correspond to observations of Secchi depths in Swiss lakes (Schwefel et al. 2016) and fall into the decreasing range of transparency from an oligotrophic to eutrophic system (Carlson 1977). For glacier-fed lakes (typical above 2000 m) rich in sedimentary material, ε_{abs} is set to 1.00 m^{-1}.

Missing forcing data within that timeframe can cause significant discrepancies in the model and needs to be properly handled. We apply different simple data patching methods depending on the data and the number of missing data. For all variables, gaps of less than one day are completed by linear interpolation. For highly seasonal variables (air temperature, solar radiation, humidity, inflow discharge, inflow temperature, light absorption), missing data are replaced by the corresponding day-of-year averages obtained from the available data. For cloud coverage, missing data are obtained as one minus the ratio between measured solar radiation and 90 % of the theoretical solar radiation. The latter is calculated as described in Appendix C.

The timeframe of the model is determined by the availability of the necessary meteorological data (air temperature, solar radiation, humidity, wind, precipitation). Initial conditions for temperature and salinity are set using conductivity-temperature-depth (CTD) profiles or using the temperature information from the closest lake. We apply different data patching methods to remove data gaps from the forcing depending on the length of the data gap. For small data gaps with duration not exceeding one day, the dataset is linearly interpolated. In total < 1 % of the dataset is corrected using this approach. Longer data gaps of up to 20 days are replaced by the long-term average values for the corresponding day of the year. Only ~ 1.5 % of the dataset is corrected using this approach.

2.3 Calibration

Model parameters are set to logical default values, and four of them are calibrated (see Table 2). The parameters to calibrateModel parameters are set to standard default values, and four of them are calibrated (see Table 2). The parameters *p_radin* and and *f_wind* scale the incoming long-wave radiation and the wind speed, respectively, and can be used to compensate for systematic differences between the meteorological conditions on the lake and at the closest meteo station. The parameter *a_seiche* determines the fraction of wind energy that feeds the internal seiches. This parameter is lake-specific, as it depends on the lake's morphology and it's exposition to different wind directions. Finally, the parameter *p_albedo* scales the albedo of ice and snow applied to incoming shortwave radiation, which depends on the ice/snow cover properties and is unknown for the individual lakes. The calibration parameters were selected according to their importance for the model (e.g. based on previous sensitivity analysis). The), and their number of parameters iswas deliberately kept small in order to maintainkeep the calibration process simple and focused. Calibration is performed using PEST v15.0 (see http://pesthomepage.org), a model-independent parameter estimation software (Doherty, 2016). As a reference for calibration, temperature observations from CTD profiles are used. Calibration is performed on a yearly basis, unless significant changes are made to either the model, the forcing data, or the observational data. For the eight lakes to which no observations are available (e.g. release of a new version of Simstrat or delivery of a large amount of new observational data). For the eight lakes without observational data, parameters are set to their default value (see Table 2) with no calibration preformedperformed, and the lack of calibration is clearly indicated on the online platform.

2.4 Output / Available data on the online platform

The online platform (accessible at https://simstrat.eawag.ch) is automatically fed every week with model results, metadata and plots for all the 54 modelled lakes (see Figure 2). It allows for efficient display and open sharing of the model results for interested users. While the framework is here restricted to Swiss lakes, the code could be easily adapted to other lakes outside Switzerland and used at the global scale. From the model results, we directly obtain time series of several model output variables (in particular. Those dataset include temperature, salinity, Brunt-Väisälä frequency, vertical diffusivity, and ice thickness).. In addition, we use the following known physical and lake-related properties: the acceleration of gravity $g = 9.81$ m^2 s^{-1}, the heat capacity of water $c_\mathrm{p} = 4.18 \cdot 10^3$ J K^{-1} kg^{-1}, the volume of the lake V [m^3], the area A_z [m^2], temperature T_z [K[°C], and density ρ_z [kg m^{-3}] at depth z [m], and the mean lake depth $\bar{z} = \frac{1}{V}\int z\ A_z\ dz$ [m]. From this, we] to calculate time series of derived values:

- Mean lake temperature: $\bar{T} = \frac{1}{V}\int T_z\, A_z\, dz$ [K[°C]

Formatted: Don't keep with next, Don't keep lines together

- Heat content: $H = c_\mathrm{p} \int \rho_z \, T_z \, A_z \, dz$ [J]
- Schmidt stability: $S_\mathrm{T} = \frac{g}{A_0} \int (z - \bar{z}) \, \rho_z \, A_z \, dz$ [J m^{-2}]
- Timing of summer stratification: we use a threshold based on the Schmidt stability to determine beginning and end of summer stratification. The lake is assumed to be stratified for $S_T / z_{lake} \geq 10$ J m^{-3}. Using a different criterion (e.g., temperature difference between surface and bottom water) results in variations in the calculated stratification period; however, the general pattern among lakes remains similar~~).~~.
- Timing of ice cover: we use the existence of ice to determine beginning and end of ice covered period.

From these results, we create static and interactive plots. The latter are created using the Plotly Python Library (see https://plot.ly/python). The plots can be categorized as follows:

- History (e.g., contour plot of the whole temperature time series, line plot of the whole time series of Schmidt stability);
- Current situation (e.g., latest temperature profile);
- Statistics (e.g., average monthly temperature profiles, long-term trends).

~~An online platform (accessible at https://simstrat.eawag.ch) is automatically weekly fed with model results, metadata and plots for all the 54 modelled lakes (see Figure 2). Such a platform allows for efficient display and sharing of the model results for interested users, and is built for straightforward application to other lakes outside Switzerland.~~

All Output and processed data are directly available from the online platform.

3 Results and discussion

~~Model~~Analysis of model output ~~data is very well-suited for comparison analyses, and studies of~~ allows to compare the response of the different systems to specific events or to long-~~-~~ term ~~change~~changes. The Simstrat model web interface provides regional long-term high-frequency data updated in near real-time as output. This represents a novel way to monitor, analyse and visualize processes in aquatic systems, and, most importantly, grant the entire community direct access to the findings. The coupling between Simstrat and PEST provides an effective way to calibrate model parameters~~ automatically.~~. The uncertainty quantification finally allows an appropriate informed use of the output data. Yet, more advanced methods for both parameter estimation and uncertainty quantification such as Bayesian inference (Gelman et al., 2013) should be ~~interfaced to Simstrat. Similarly, the simple data patching applied for missing input data would benefit from state of the art data science methods in the future.~~applied to Simstrat.

Out of the 46 calibrated lakes, the post-calibration root mean square error (RMSE) is < 1 °C for 17 lakes, between 1 and 1.5 °C for 15 lakes, between 1.5 and 2 °C for 8 lakes and ~~>~~between 2 °C and 3°C for 6 lakes (Figure 3~~).~~), calibration data was not sufficient for 8 lakes in which we used standard settings. This is comparable to the RMSE range of ~0.7-2.1 °C reported in a recent global 32-lake modelling study using GLM (Bruce et al., 2018)~~.~~

also including Lake Geneva, Lake Constance and Lake Zurich. The correlation coefficient remains always higher than 0.93 suggesting also that the model successfully reproduce the thermal structure of the investigated lakes Overall, the quality of the

Formatted: Heading 3

results is better for lowland lakes than for high altitude lakes where local meteorological and watershed information are often missing.

We illustrate the potential of high-frequency lake model data with two examples: first by briefly showing the long-term changes caused by climate change in Lake Brienz (section 3.1), and secondly by investigating the differential response of lakes across Switzerland to episodic forcing (short-term extremes, section 3.2).

3.1 Long-term evolution of the thermal structure of lakes, in response to climate trends.

Lake Brienz (https://simstrat.eawag.ch/LakeBrienz, Figure 2) situated in central Switzerland at 564 m asl is a typical deep (259 m) oligotrophic peri-alpine lake with a retention time of 2.6 years (Wüest et al., 2007). The effect of the upstream hydropower operation were previously shown to shift riverine particle inputs from summer to winter in this lake (Finger et al., 2006, 2007). Changes in the lake thermal structure from modifications of riverine particle inputs and discharge regime in a context of climate warming was recently quantified for nearby Lake Biel and Lake Geneva (Råman Vinnå et al., 2018).

Over the period 1981–2015, we observe an increase in both yearly averaged surface and bottom temperatures with significant ($p<0.001$) trends of +0.64 °C/decade and +0.11 °C/decade respectively (Figure 4a). Analysis from in situ observation for the same period indicates a trend for the surface temperature around 0.72 °C/decade ($p\sim0.07$). This is in line with epilimnion/hypolimnion trends observed in neighbouring deep lakes ranging from +0.22/+0.11 °C/decade in Lake Geneva (Lemmin and Amouroux, 2006) to +0.41/+0.13 °C/decade inOver the period 1981–2015, yearly averaged simulated surface temperatures in Lake Brienz increased with a significant ($p<0.001$) trend of +0.69 °C/decade (Figure 4a). For the same period, monthly in situ observations indicate a similar trend of 0.72 °C/decade ($p\sim0.07$), while the trend of air temperature at the meteorological station in Interlaken is lower (+0.50 °C/decade, $p<0.01$). Based on physical principles, lake surface temperature is expected to increase less than air temperature (Schmid et al., 2014), however Schmid and Köster (2016) also observed a higher trend in lake surface temperature than in air temperature for Lower Lake Zurich and assigned the excess warming to a positive trend in solar radiation. For the period 1981-2015, the trend in solar radiation is 5 W/m^2/decade that corresponds to an equilibrium temperature increase of about 0.2°C/decade. The warming rate at the surface of Lake Brienz is larger than observed trends in neighbouring lakes with reported increases of +0.46 °C/decade for Upper Lake Constance (1984 – 2011, Fink et al. 2014), +0.41°C/decade for Lower Lake Zürich (1981 - 2013, Schmid and Köster, 2016; 1955 - 2013, Livingstone, 2003). The vertical heterogeneous heating observed in Lake Brienz is also consistent with previous observations showing that difference in warming between the surface and the bottom increase the strength and length, +0.55°C/decade for Lower Lake Lugano (1972 – 2013, Lepori and Roberts, 2015). This can be explained by the lower light penetration in Lake Brienz (ranging from ~1 m to ~10 m) compared to other light; the increase in solar radiation being distributed into a shallower layer and thereby warming slightly more the lake surface.

The temperature increase was significantly smaller in the hypolimnion, with a minimum trend at the lake bottom of 0.16 °C/decade ($p<0.001$), leading to a depth-averaged rate of temperature increase of 0.22 °C/decade ($p<0.001$). The temperature difference between the inflow and the outflow also contributes to the heat budget. While no significant change in the yearly total discharge was observed at the gauging stations of FOEN for the inflows Aare and Lütschine for the period 1981 – 2015, the weighted inflow temperature increased by 0.26 °C/decade. The riverine temperature remains colder than the lake surface temperature leading to a yearly average loss of energy by through-flow of ~ - 40 W/m^2 for 2015. This result is consistent with the recent observations of Råman Vinnå (2018) suggesting that tributaries significantly affect the thermal response of lakes with residence time up to 2.7 years (as Lake Brienz). The contribution of the river to the heat budget of Lake Brienz is also ~ 4 times larger than that previously estimated for Upper Lake Constance (Fink et al. 1994), a lake with a longer residence time. The increasing difference over time between the inflow temperature and the outflow temperature (taken as the lake surface temperature) leads to a non-negligible cooling contribution from the river of ~ 0.14 °C/decade ($p<0.05$). The temporal change in the discharge and its temperature resulting from climate change should therefore be taken into account in predicting the change in lake thermal structure.

The vertically heterogeneous warming modelled in Lake Brienz is consistent with previous observations showing that the difference in warming between the surface and the bottom increases the strength and duration of the stratified period (Zhong et al., 2016; Wahl and Peeters, 2014). We ~~detect~~simulate an earlier onset of the stratification in spring of -7.5 day/decade ($p<0.001$) and a later breakdown of the stratification by +3.7 day/decade ($p<0.001$) (Figure 4c). Both the warming trend and the increase in length of the stratified period increase the Schmid stability (Figure ~~4e) and heat content (Figure 4f). The increase of Lake Brienz heat content amounts to ~2·10^{16} J over 38 years, which corresponds to roughly two thirds of the heat extraction potential for this lake (Gaudard et al., 2019). Contrarily to the above-described variables, no clear trend was detectable in the yearly maximum stratification strength (Brunt-Väisälä frequency, Figure 4d).~~4d) and heat content (Figure 4f). Finally, the yearly maximum stratification strength (Brunt-Väisälä frequency, Figure 4e) gradual increases over the investigated period with a rate of 3.3 x 10^{-4} s^{-2}/decade. The simulated increase in overall stability (Figures 4d, 4e and 4f) reduces vertical mixing and affects the vertical storage of heat with less heat transferred immediately below the thermocline causing a slight decrease in temperature observed in autumn at ~30 m depth (Figure 4b). This effect is even more clearly seen in other lakes like Lake Geneva (https://simstrat.eawag.ch/LakeGeneva) with the surface waters warming strongly (+1 °C/decade in June), resulting in a cooling layer between 20 and 60 m (-0.2 °C/decade) in late summer. Such a reduction of vertical exchange is self-strengthening and enhances the differential vertical warming.

~~The observed increase in overall stability (Figures 4c and 4e) reduces vertical mixing and affects the vertical storage of heat with less heat transferred immediately below the thermocline (Figure 4b) with a slight decrease in temperature observed in autumn at ~30 m depth. Additionally, this effect is clearly seen in Lake Geneva (Figure 5, https://simstrat.eawag.ch/LakeGeneva) with the surface waters warming strongly (+1 °C/decade in June), resulting in a cooling~~

~~layer between 20 and 60 m (-0.2 °C/decade) in late summer.~~ Such ~~reduction of vertical exchange is self-strengthening and enhances the vertical differential warming.~~

~~Similar analysis was repeated for~~analyses can be extended to all ~~the~~ modelled lakes~~: an~~. An inter-comparison of the temporal extent of ~~both~~ summer ~~and winter~~ stratification and winter ice cover period is illustrated in Figure ~~6~~5. An altitude-dependent decrease of the duration of summer stratification is observed, along with a stronger corresponding increase in the duration of the inverse winter stratification from 1200 m ~~asl~~. a.s.l. This is possibly linked to an altitude dependency of climate-driven warming in Swiss lakes, first reported by Livingstone et al. (2005)~~,~~, which may be caused by a delay in meltwater runoff (Sadro et al., 2018). Here this process is not directly resolved but incorporated through the calibration procedure spanning all seasons.

In conclusion, the online platform provides all the data to estimate the past rate of warming of lakes and evaluate how the different external processes contribute to their heat budgets. The change in the thermal structure depends mostly to the change in atmospheric forcing, yet, other factors such as the changes in discharge and temperature from the tributaries and the light absorption into the lake should also be taken into account. We specifically show that the rate of warming of the lake surface temperature significantly differs from that of depth-averaged temperature, thereby highlighting the benefit of using either *in-situ* observations resolving the thermal structure over the water column or hydrodynamic model output for assessing climate change impacts on lake thermal structure.

3.2 Event based evolution of the lake thermal structure.

A major drawback of traditional lake monitoring programs in Switzerland is the coarse temporal resolution, with measurements often performed on a monthly basis. Thought sufficient for direct long-term trend studies as shown in section 3.1 when conducted over ~~long~~an extended period typically longer than 30 years (Gray et al., 2018)~~,~~. However, traditional monitoring programs cannot resolve the impact of short-term events and their consequences for the ecosystem. This is ~~however~~ a strength of high-frequency (hourly time scale) lake modelling, which allows for simulation and comparison of the effects associated with rapid and often ~~brutal~~severe events such as storms. Based on high-frequency observations, Woolway et al. (2018) showed the effects of a major storm on Lake Windermere. They observed a decrease in the strength of the stratification, a deepening of the thermocline and the onset of internal waves oscillations ultimately upwelling oxygen depleted cold water into the downstream river. Furthermore, Perga et al. (2018) illustrated how storms could be just as important as gradual long-term trends for changes in light penetration and thermal structure in an Alpine lake.

Here we demonstrate how high-frequency model output can be used to study the influence of specific events on the thermal dynamics of lakes. As an example, we focus on the 28th of June 2018 when Switzerland experienced a strong but by no means exceptional storm with ~~Northern~~Northeasterly winds mainly affecting the North-Western part of the country – the mean wind speed during that day is shown spatially in Figure ~~7a~~6a. The evolution of the stratification strength, illustrated here by the

Schmidt stability, is given in Figure ~~7b~~6b for one of the most affected lakes, Lake Neuchâtel (https://simstrat.eawag.ch/LakeNeuchatel, Figure 2). This lake, with the main axis well-aligned to synoptical winds, experienced a ~8 % decrease in the Schmidt stability over this half-day event. Yet, the effects were not long-lasting and the Schmidt stability reverted to its pre-storm value within ~5 days (Figure ~~7b~~6b). This also resulted in a total increase of the lake heat content by ~$1.4 \cdot 10^{16}$ J from the start of the storm to the time of recovery. We used the Schmidt stability recovery duration as a way to assess the short-term effect of the storm on the different modelled lakes. In Figure ~~7a~~6a, lakes are coloured based on the delay in Schmidt stability increase (in days) caused by the storm. The impact of the storm was ~~obviously~~ not limited to Lake Neuchâtel but rather showed a regionally-varying pattern. Particularly small- to medium-sized lakes in the North-Western parts of Switzerland were more affected than large lakes or lakes located in the Southern part of Switzerland. However, the thermal structure of ~~the~~these lakes quickly reverted to the seasonal ~~spring~~early summer warming trend.

So far, climate-driven warming has been recognized to cause an overall increase in lake stratification strength and duration, and a gradual warming of the different layers (Schwefel et al., 2016; Zhong et al., 2016; Wahl and Peeters, 2014). Air temperature trend was the most studied forcing parameter. Yet, the dynamics of extreme events (such as heat waves, drought spells, storms), including their changes in strength and distribution, has been comparatively overlooked. Scenario exploration, climate change studies, or historical forcing reanalysis should be integrated in such web-based hydrodynamic platforms to assess their roles in modifying the lake thermal structures and heat storage.

4 Conclusion

The workflow presented in this paper allows open sharing of high-frequency, up-to-date and permanently available lake model results for multiple users and purposes. ~~These~~We demonstrated the benefit of the platform through two simple case studies. First, we showed that the high frequency modelled temperature data allows a complete assessment of the effect of climate change on the thermal structure of a lake. We specifically show the need to evaluate changes in all atmospheric forcing, in the watershed or through-flow heat energy and in light penetration to accurately assess the evolution of the lake thermal structure. Then we showed that the high frequency modelled data can be used to investigate special events such as wind storms, there in-situ measurements under current temporal resolution are failing. More generally, these results are well suited for the following applications and target groups:

- For the public, the platform serves as an informative website enabling easy access to broad quantities of regional scientific results, with the intention of raising interest about lake ecosystem dynamics.
- For lake managers, the platform makes relevant information available, such as (i) ~~current~~near real time temperature and stratification conditions of the lakes, (ii) simple statistical analyses such as monthly temperature profiles and long-term temperature trends.

Formatted: Indent: Left: 0.63 cm, Hanging: 0.63 cm, Line spacing: 1.5 lines

- For researchers, this work can facilitate (i) scenario modelling of any of the lakes, as the basic model setup is ready-to-use, (ii) improvement of the lake model with addition of previously unresolved processes (e.g., ~~ice cover and river intrusion~~resuspension with changed light properties), (iii) access to variables that were previously not or irregularly available (e.g., vertical diffusivity, heat content, stratification and heat fluxes), and (iv) specific comparative analyses, whereby a given question can be investigated simultaneously over many lakes (e.g., the impact of climate change~~).~~ or a regional storm).

By promoting a cross-exchange of expertise through openly sharing of in-situ and model data at high frequency, this open-access data platform is a new path forward for scientists and practitioners.

Formatted: Normal, Line spacing: single, No bullets or numbering

Code and data availability

The workflow was developed for Swiss lakes but can be easily extended to other geographical area or at global scale by using other meteorological input data. Simstrat and the Python workflow are available on https://github.com/Eawag-AppliedSystemAnalysis/Simstrat/releases/tag/v2.1 (https://doi.org/10.5281/zenodo.2600709) and https://github.com/Eawag-AppliedSystemAnalysis/Simstrat-WorkflowModellingSwissLakes (https://doi.org/10.5281/zenodo.2607153). Meteorological data are available from MeteoSwiss (https://gate.meteoswiss.ch/idaweb/), hydrological data are available from FOEN (https://www.hydrodaten.admin.ch), CTD data were provided by various sources listed here: https://simstrat.eawag.ch/impressum . The calibration software PEST is available on http://www.pesthomepage.org/

Formatted: English (United Kingdom)

Formatted: English (United Kingdom)

Author contribution

The new version of Simstrat was developed by FB, AG and LRV. The workflow was developed by AG. The ice model was developed by LVR. The concept of the workflow was defined by DB. All authors contributed to the validation of the model and interpretation of the results. AG and DB wrote the manuscript with contributions from FB, LVR and MS.

Competing interests

The authors declare that they have no conflict of interest

Acknowledgment

We thank Davide Vanzo for helping with the Docker and the scripts and Michael Pantic for helping restructuring the version 2.1 of Simstrat. We finally thank Marie-Elodie Perga for her comments on a preliminary version of the manuscript. The full list of ~~acknowledgement~~acknowledgements regarding in-situ observations can be found here: https://simstrat.eawag.ch/impressum .

References

Antenucci, J. and Imerito, A.: The CWR dynamic reservoir simulation model DYRESM, Science Manual, The University of Western Australia, Perth, Australia., 2000.

Bruce, L. C., Frassl, M. A., Arhonditsis, G. B., Gal, G., Hamilton, D. P., Hanson, P. C., Hetherington, A. L., Melack, J. M., Read, J. S., Rinke, K., Rigosi, A., Trolle, D., Winslow, L., Adrian, R., Ayala, A. I., Bocaniov, S. A., Boehrer, B., Boon, C., Brookes, J. D., Bueche, T., Busch, B. D., Copetti, D., Cortés, A., de Eyto, E., Elliott, J. A., Gallina, N., Gilboa, Y., Guyennon, N., Huang, L., Kerimoglu, O., Lenters, J. D., MacIntyre, S., Makler-Pick, V., McBride, C. G., Moreira, S., Özkundakci, D., Pilotti, M., Rueda, F. J., Rusak, J. A., Samal, N. R., Schmid, M., Shatwell, T., Snorthheim, C., Soulignac, F., Valerio, G., van der Linden, L., Vetter, M., Vinçon-Leite, B., Wang, J., Weber, M., Wickramaratne, C., Woolway, R. I., Yao, H. and Hipsey, M. R.: A multi-lake comparative analysis of the General Lake Model (GLM): Stress-testing across a global observatory network, Environmental Modelling & Software, 102, 274–291, doi:10.1016/j.envsoft.2017.11.016, 2018.

Burchard, H., Bolding, K. and Villarreal, M. R.: GOTM, a general ocean turbulence model: theory, implementation and test cases, Space Applications Institute., 1999.

Carlson, R. E: A trophic state index for lakes. Limnology and Oceanography. 22(2). 361-369, 1977

Doherty, J.: PEST: Model-Independent Parameter Estimation, 6th ed., Watermark Numerical Computing, Australia., 2016.

Finger, D., Schmid, M. and Wüest, A.: Effects of upstream hydropower operation on riverine particle transport and turbidity in downstream lakes, Water Resources Research, 42(8), doi:10.1029/2005WR004751, 2006.

Finger, D., Bossard, P., Schmid, M., Jaun, L., Müller, B., Steiner, D., Schäffer, E., Zeh, M. and Wüest, A.: Effects of alpine hydropower operations on primary production in a downstream lake, Aquat. Sci., 69(2), 240–256, doi:10.1007/s00027-007-0873-6, 2007.

Fink, G., Schmid, M., Wahl, B., Wolf, T., & Wüest, A. (2014). Heat flux modifications related to climate-induced warming of large European lakes. Water Resources Research, 50(3), 2072-2085.

Gaudard, A., Schwefel, R., Råman Vinnå, L., Schmid, M., Wüest, A. and Bouffard, D.: Optimizing the parameterization of deep mixing and internal seiches in one-dimensional hydrodynamic models: A case study with Simstrat v1.3, Geosci. Model Dev., 10(9), 3411–3423, doi:10.5194/gmd-10-3411-2017, 2017.

Gaudard, A., Wüest, A. and Schmid, M.: Using lakes and rivers for extraction and disposal of heat: Estimate of regional potentials, Renewable Energy, 134, 330–342, doi:10.1016/j.renene.2018.10.095, 2019.

Gelman, A., Carlin, J., Stern, H. and Rubin, D.: Bayesian Data Analysis, 3rd ed., Chapman and Hall/CRC, New York., 2013.

Gill, A. E.: Atmosphere-Ocean Dynamics, Academic Press, San Diego, California, USA. [online] Available from: http://books.google.ch/books?hl=de&lr=&id=8kFPh_SvnAIC&oi=fnd&pg=PP2&dq=Atmosphere-Ocean+dynamics&ots=B77L2z3Shp&sig=6rVJ55ftAUHkMDEC_NzBEgkL2Lw (Accessed 31 January 2014), 1982.

Goudsmit, G.-H., Burchard, H., Peeters, F. and Wüest, A.: Application of k-ϵ turbulence models to enclosed basins: The role of internal seiches, Journal of Geophysical Research: Oceans, 107(C12), 3230, doi:10.1029/2001JC000954, 2002.

Gray, D. K., Hampton, S. E., O'Reilly, C. M., Sharma, S. and Cohen, R. S.: How do data collection and processing methods impact the accuracy of long-term trend estimation in lake surface-water temperatures?, Limnology and Oceanography: Methods, 16(8), 504–515, doi:10.1002/lom3.10262, 2018.

Hamilton, D. P., Carey, C. C., Arvola, L., Arzberger, P., Brewer, C., Cole, J. J., Gaiser, E., Hanson, P. C., Ibelings, B. W., Jennings, E., Kratz, T. K., Lin, F.-P., McBride, C. G., Marques, M. D. de, Muraoka, K., Nishri, A., Qin, B., Read, J. S., Rose, K. C., Ryder, E., Weathers, K. C., Zhu, G., Trolle, D. and Brookes, J. D.: A Global Lake Ecological Observatory Network (GLEON) for synthesising high-frequency sensor data for validation of deterministic ecological models, Inland Waters, 5(1), 49–56, doi:10.5268/IW-5.1.566, 2015.

Hipsey, M. R., Bruce, L. C. and Hamilton, D. P.: GLM - General Lake Model. Model overview and user information, Technical Manual, The University of Western Australia, Perth, Australia. [online] Available from: http://swan.science.uwa.edu.au/downloads/AED_GLM_v2_0b0_20141025.pdf, 2014.

Jennings, E., Eyto, E., Laas, A., Pierson, D., Mircheva, G., Naumoski, A., Clarke, A., Healy, M., Šumberová, K. and Langenhaun, D.: The NETLAKE MetadatabaseMetadatabae—A Tool to Support Automatic Monitoring on Lakes in Europe and Beyond, Limnology and Oceanography Bulletin, 26(4), 95–100, doi:10.1002/lob.10210, 2017.

Kiefer, I., Odermatt, D., Anneville, O., Wüest, A. and Bouffard, D.: Application of remote sensing for the optimization of in-situ sampling for monitoring of phytoplankton abundance in a large lake, Sci. Total Environ., 527–528, 493–506, doi:10.1016/j.scitotenv.2015.05.011, 2015.

Lemmin, U. and Amouroux, A.: The influence of climate change on Lake Geneva, SIL Proceedings, 1922-2010, 29(4), 1806–1810, doi:10.1080/03680770.2006.11903000, 2006.

Lepori, F., and Roberts, J. J.: Past and future warming of a deep European lake (Lake Lugano): What are the climatic drivers?. J Great Lakes Res 41.4 (2015): 973-981.

Leppäranta, M.: Modelling the Formation and Decay of Lake Ice, in The Impact of Climate Change on European Lakes, edited by G. George, pp. 63–83, Springer Netherlands, Dordrecht., 2010.

Leppäranta, M.: Freezing of lakes and the evolution of their ice cover, Springer, New York., 2014.

Livingstone, D. M.: Impact of secular climate change on the thermal structure of a large temperate central European lake, Climatic change, 57(1–2), 205–225, 2003.

Livingstone, D. M., Lotter, A. F. and Kettle, H.: Altitude-dependent differences in the primary physical response of mountain lakes to climatic forcing, Limnology and Oceanography, 50(4), 1313–1325, 2005.

Meyers, T. P. and Dale, R. F.: Predicting Daily Insolation with Hourly Cloud Height and Coverage, J. Climate Appl. Meteor., 22(4), 537–545, doi:10.1175/1520-0450(1983)022<0537:PDIWHC>2.0.CO;2, 1983.

Mironov, D. V.: Parameterization of lakes in numerical weather prediction. Part 1: Description of a lake model, German Weather Service, Offenbach am Main, Germany., 2005.

Perga, M.-E., Bruel, R., Rodriguez, L., Guénand, Y. and Bouffard, D.: Storm impacts on alpine lakes: Antecedent weather conditions matter more than the event intensity, Glob Chang Biol, 24(10), 5004–5016, doi:10.1111/gcb.14384, 2018a.

Perroud, M., Goyette, S., Martynov, A., Beniston, M. and Anneville, O.: Simulation of multiannual thermal profiles in deep Lake Geneva: A comparison of one-dimensional lake models, Limnology and Oceanography, 54(5), 1574–1594, 2009.

Poole, H. H. and Atkins, W. R. G.: Photo-electric measurements of submarine illumination throughout the year, Journal of the Marine Biological Association of the United Kingdom, 16(1), 297–324, 1929.

Råman Vinnå, L., Wüest, A., Zappa, M., Fink, G. and Bouffard, D.: Tributaries affect the thermal response of lakes to climate change, Hydrol. Earth Syst. Sci., 22(1), 31–51, doi:10.5194/hess-22-31-2018, 2018.

Riley, M. J. and Stefan, H. G.: Minlake: A dynamic lake water quality simulation model, Ecological Modelling, 43(3), 155–182, doi:10.1016/0304-3800(88)90002-6, 1988.

Sadro, S., Sickman, J. O., Melack, J. M. and Skeen, K.: Effects of Climate Variability on Snowmelt and Implications for Organic Matter in a High-Elevation Lake, Water Resources Research, 54(7), 4563–4578, doi:10.1029/2017WR022163, 2018.

Saloranta, T. M.: Modeling the evolution of snow, snow ice and ice in the Baltic Sea, Tellus A, 52(1), 93–108, doi:10.1034/j.1600-0870.2000.520107.x, 2000.

Saloranta, T. M. and Andersen, T.: MyLake—A multi-year lake simulation model code suitable for uncertainty and sensitivity analysis simulations, Ecological Modelling, 207(1), 45–60, 2007.

Schmid M, Hunziker S, Wüest A (2014). Lake surface temperatures in a changing climate: a global perspective, Climatic Change, 124, 301-305

Schmid, M. and Köster, O.: Excess warming of a Central European lake driven by solar brightening, Water Resour. Res., 52(10), 8103–8116, doi:10.1002/2016WR018651, 2016.

Schwefel, R., Gaudard, A., Wüest, A. and Bouffard, D.: Effects of climate change on deep-water oxygen and winter mixing in a deep lake (Lake Geneva)–Comparing observational findings and modeling, Water Resources Research, 52(11), 8811–8826, doi:10.1002/2016WR019194, 2016.

Smith, W. L.: Note on the Relationship Between Total Precipitable Water and Surface Dew Point, J. Appl. Meteor., 5(5), 726–727, doi:10.1175/1520-0450(1966)005<0726:NOTRBT>2.0.CO;2, 1966.

Stepanenko, V. M., Mammarella, I., Ojala, A., Miettinen, H., Lykosov, V. and Vesala, T.: LAKE 2.0: a model for temperature, methane, carbon dioxide and oxygen dynamics in lakes, Geosci. Model Dev., 9(5), 1977–2006, doi:10.5194/gmd-9-1977-2016, 2016.

Thiery, W., Stepanenko, V. M., Fang, X., Jöhnk, K. D., Li, Z., Martynov, A., Perroud, M., Subin, Z. M., Darchambeau, F., Mironov, D. V. and others: LakeMIP Kivu: evaluating the representation of a large, deep tropical lake by a set of one-dimensional lake models, Tellus A: Dynamic Meteorology and Oceanography, 66(1), 21390, doi:10.3402/tellusa.v66.21390, 2014.

Wahl, B. and Peeters, F.: Effect of climatic changes on stratification and deep-water renewal in Lake Constance assessed by sensitivity studies with a 3D hydrodynamic model, Limnology and Oceanography, 59(3), 1035–1052, doi:10.4319/lo.2014.59.3.1035, 2014.

Woolway, R. I., Simpson, J. H., Spiby, D., Feuchtmayr, H., Powell, B. and Maberly, S. C.: Physical and chemical impacts of a major storm on a temperate lake: a taste of things to come?, Climatic Change, 151(2), 333–347, doi:10.1007/s10584-018-2302-3, 2018.

Wüest, A., Zeh, M. and Ackerman, J. D.: Lake Brienz Project: An interdisciplinary catchment-to-lake study, Aquat. Sci., 69(2), 173–178, doi:10.1007/s00027-007-0016-0, 2007.

Yen, Y. C.: Review of thermal properties of snow, ice and sea ice, Cold Regions Research and Engineering Laboratory, Hanover, New Hampshire., 1981.

Zhong, Y., Notaro, M., Vavrus, S. J. and Foster, M. J.: Recent accelerated warming of the Laurentian Great Lakes: Physical drivers, Limnology and Oceanography, 61, 1762–1786, doi:10.1002/lno.10331, 2016.

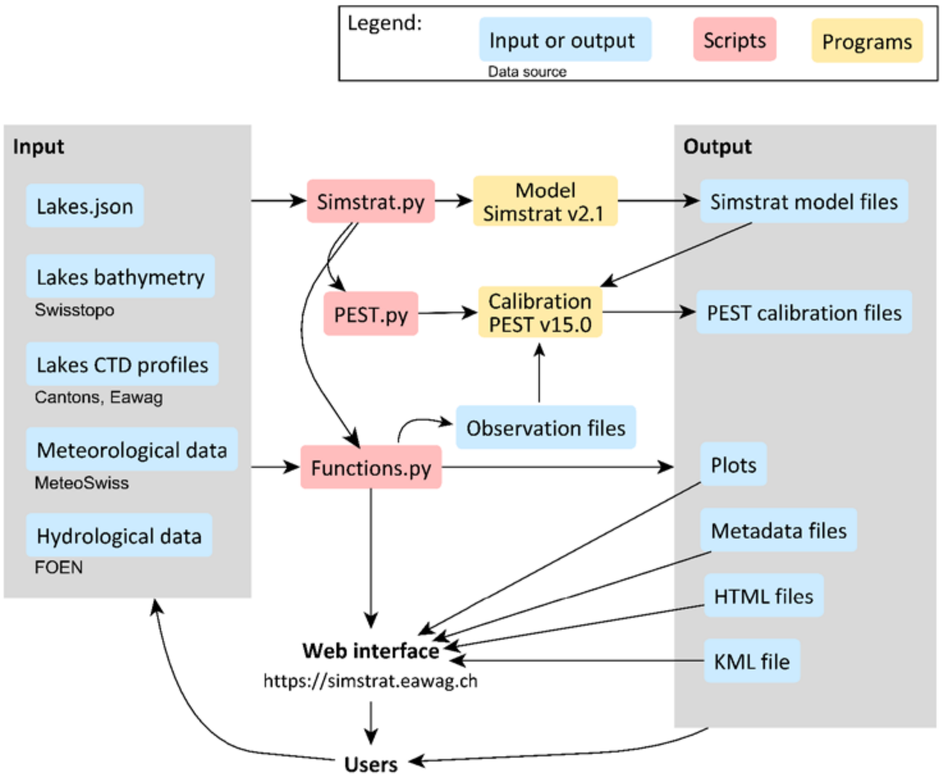

Figure 1. General workflow diagram. Model input ~~data~~ (left box) is retrieved and processed by the Python script "Simstrat.py", which runs the model (Simstrat v2.~~0~~1) and/or model calibration (using PEST v15.0) and produces output (right box). This output is then uploaded to a web interface (https://simstrat.eawag.ch) for general use. All scripts and programs are available on https://github.com/Eawag-AppliedSystemAnalysis/Simstrat/releases/tag/v2.1 and https://github.com/Eawag-AppliedSystemAnalysis/Simstrat-WorkflowModellingSwissLakes ~~.~~. Simstrat = one dimensional hydrodynamic model; CTD = Conductivity, Temperature, Depth profiler; PEST = Model independent parameter estimation and uncertainty analysis software; FOEN = Swiss Federal Office of Environment; MeteoSwiss = Swiss Federal Office of Meteorology and Climatology; Swisstopo = Swiss Federal Office of Topography

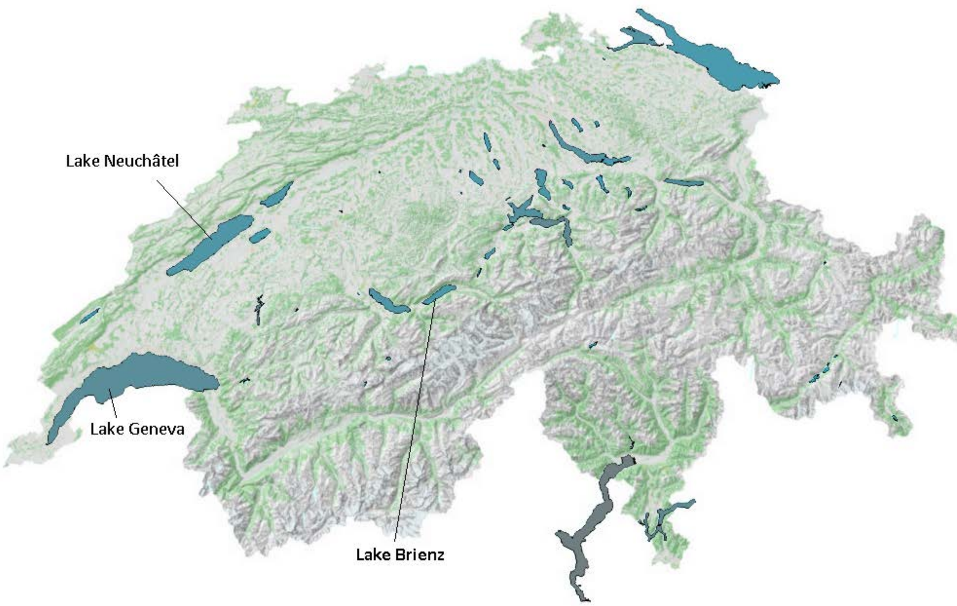
Lake Neuchâtel
Lake Geneva
Lake Brienz

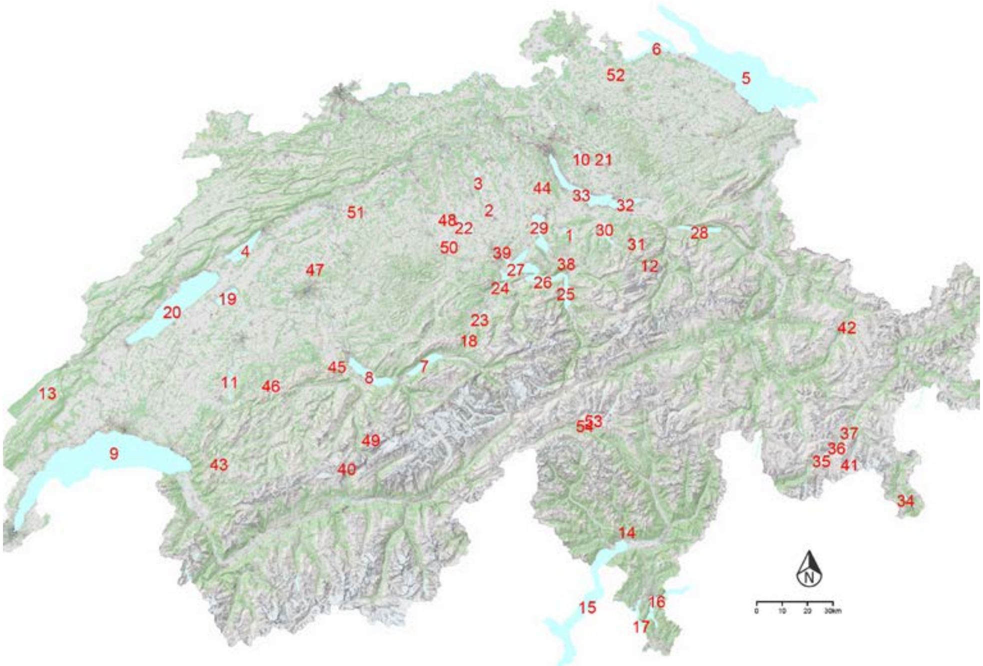

Figure 2. ~~**Snapshop**~~**Illustration of the interactive map displayed on the homepage of the online platform: https://simstrat.eawag.ch.** ~~**Status on December 4th, 2018 (3D view).**~~ **The location of the lakes discussed in this manuscript is also indicated**~~**.**~~ **with numbers (See Appendix A). Basemap is provided by Swisstopo and the specific legend can be found here https://api3.geo.admin.ch/static/images/legends/ch.swisstopo.swisstlm3d-karte-farbe_en_big.pdf**

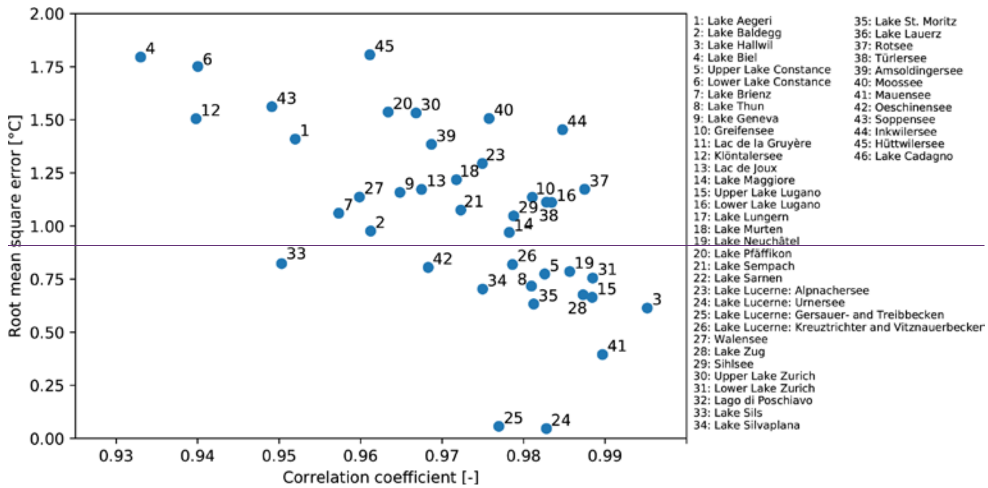
Root mean square error [°C]
2.00
1.75
1.50
1.25
1.00
0.75
0.50
0.25
0.00
0.93
0.94
0.95
0.96
0.97
0.98
0.99
Correlation coefficient [-]
1: Lake Aegeri
2: Lake Baldegg
3: Lake Hallwil
4: Lake Biel
5: Upper Lake Constance
6: Lower Lake Constance
7: Lake Brienz
8: Lake Thun
9: Lake Geneva
10: Greifensee
11: Lac de la Gruyère
12: Klöntalersee
13: Lac de Joux
14: Lake Maggiore
15: Upper Lake Lugano
16: Lower Lake Lugano
17: Lake Lungern
18: Lake Murten
19: Lake Neuchâtel
20: Lake Pfäffikon
21: Lake Sempach
22: Lake Sarnen
23: Lake Lucerne: Alpnachersee
24: Lake Lucerne: Urnersee
25: Lake Lucerne: Gersauer- and Treibbecken
26: Lake Lucerne: Kreuztrichter and Vitznauerbecken
27: Walensee
28: Lake Zug
29: Sihlsee
30: Upper Lake Zurich
31: Lower Lake Zurich
32: Lago di Poschiavo
33: Lake Sils
34: Lake Silvaplana
35: Lake St. Moritz
36: Lake Lauerz
37: Rotsee
38: Türlersee
39: Amsoldingersee
40: Moossee
41: Mauensee
42: Oeschinensee
43: Soppensee
44: Inkwilersee
45: Hüttwilersee
46: Lake Cadagno

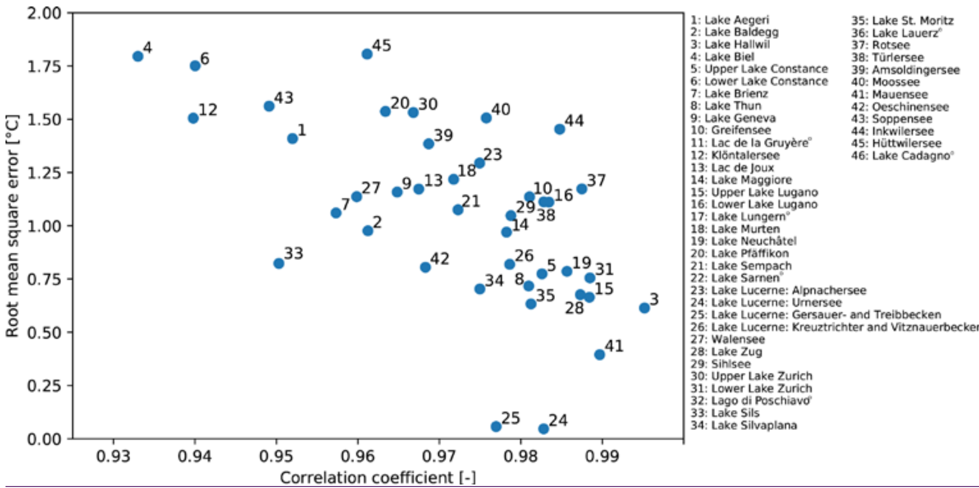

Figure 3. Performance of the model for the different lakes, as shown by the root mean square error (RMSE) and the correlation coefficient. Six lakes (with symbol ° on the legend) with RMSE > 2 °C are not shown.

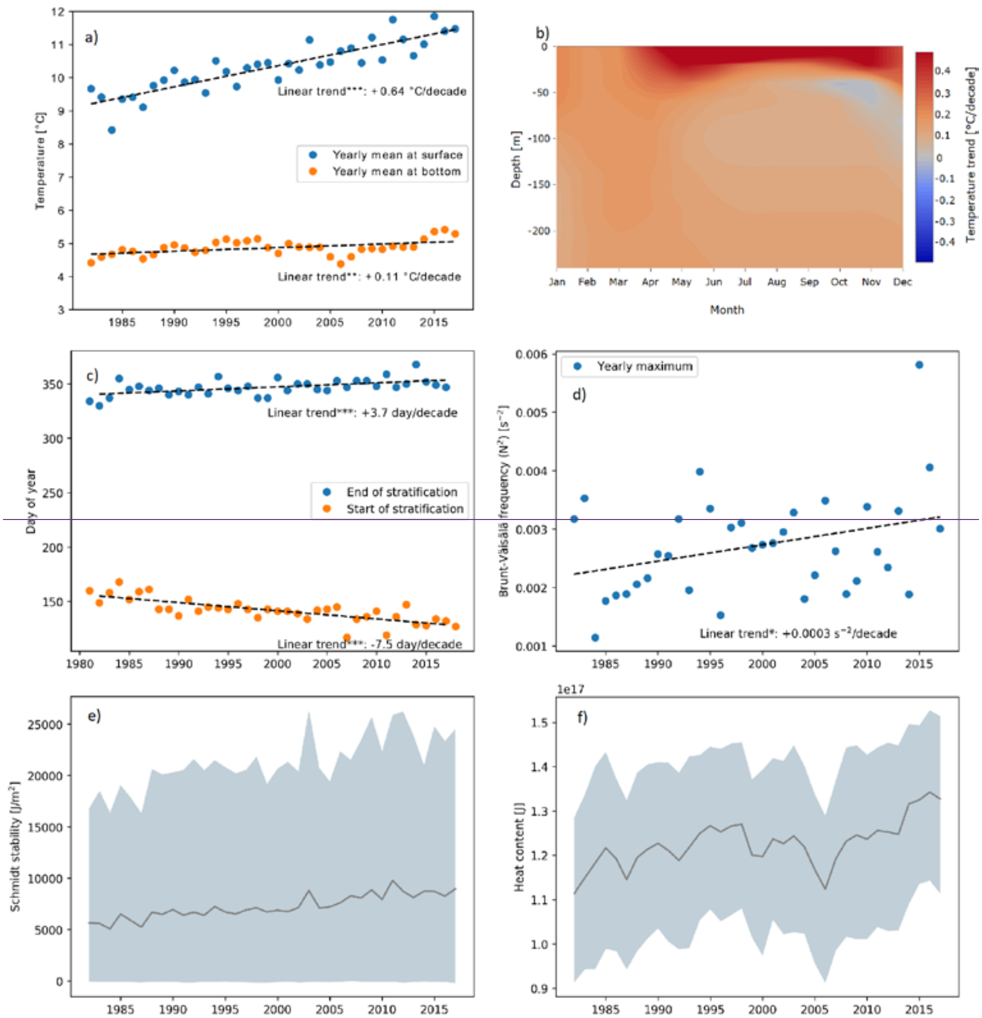
a)
Temperature [°C]
Linear trend***: +0.64 °C/decade
Yearly mean at surface
Yearly mean at bottom
Linear trend**: +0.11 °C/decade
b)
Depth [m]
Month
Temperature trend [°C/decade]
c)
Day of year
Linear trend***: +3.7 day/decade
End of stratification
Start of stratification
Linear trend***: -7.5 day/decade
d)
Yearly maximum
Brunt-Väisälä frequency (N²) [s⁻²]
Linear trend*: +0.0003 s⁻²/decade
e)
Schmidt stability [J/m²]
f)
Heat content [J]
1e17

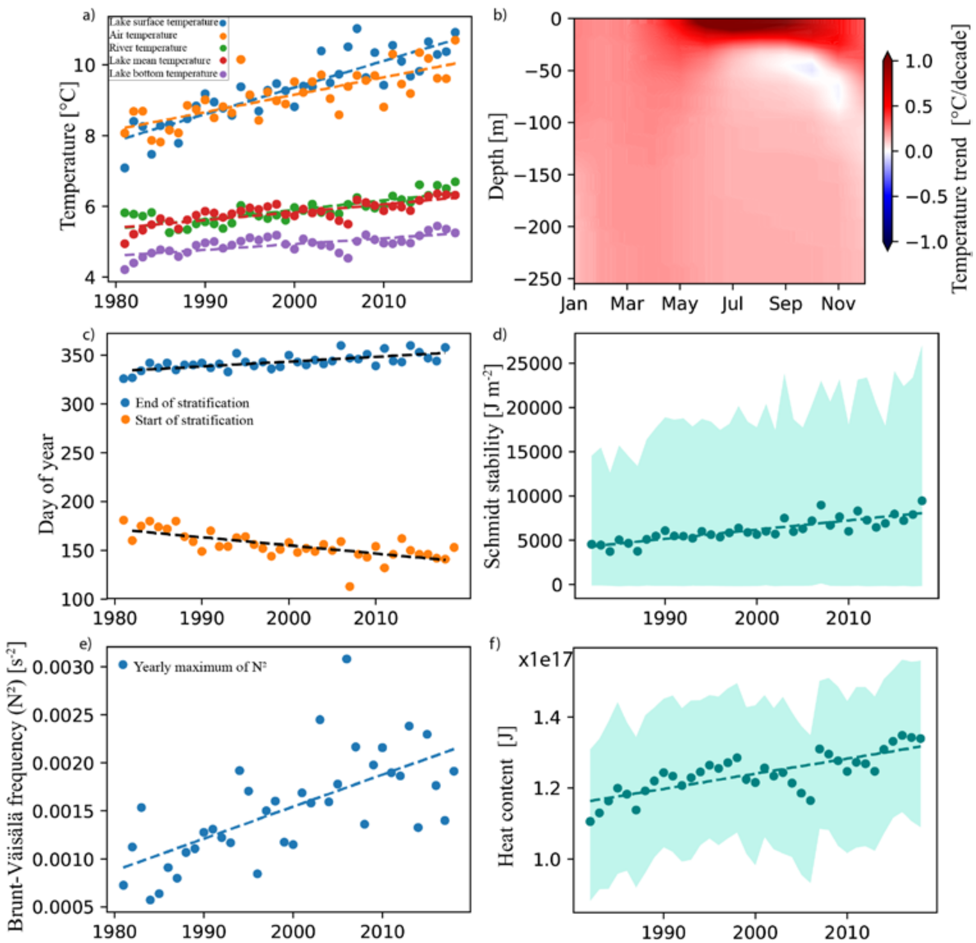

Figure 4. Evolution of several indicators for Lake Brienz over the period 1981-2018; all linear regression have p_values << 0.001: (a) yearly mean lake surface temperature (0.69 °C/decade), yearly mean air temperatures (0.49 °C/decade), yearly mean tributary temperatures (0.26 °C/decade), yearly mean lake temperatures (0.22 °C/decade) and yearly mean bottom temperatures~~,~~ (0.16 °C/decade), with linear regression, (b) contour plot of the linear temperature trend through depth and month, (c) yearly start (+3.7 days/decade) and end (-7.5 days/decade) day of summer stratification, with linear regression, (d) ~~yearly maximum Brunt-Väisälä frequency, with linear regression, (e)~~ yearly mean (line), min and max (shaded area) Schmidt stability, with linear regression,

(e) yearly maximum Brunt-Väisälä frequency ($3.3x10^{-4}$ $1/s^2$/decade), with linear regression (f) yearly mean (line), min and max (shaded area) heat content. The asterisks indicate the p-value of the linear trend: * for $p<0.001$, ** for $p<0.01$, and * for $p<0.05$.**

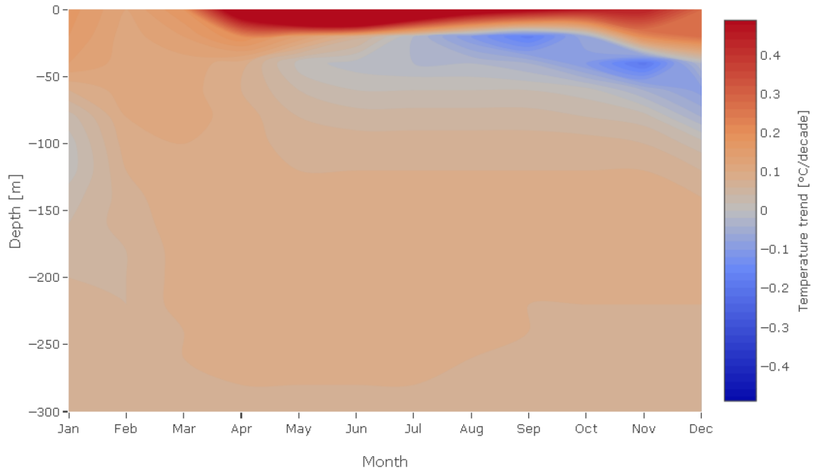

~~**Figure 5. Vertical and seasonal temperature trends modelled in Lake Geneva over the period 1981-2018. Values are given on a monthly basis.**~~

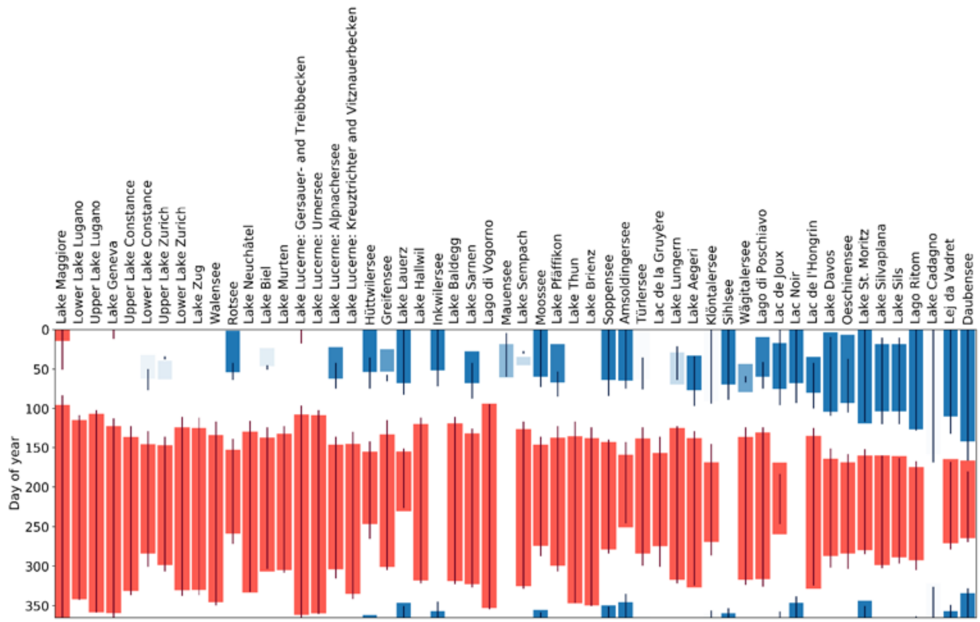
Day of year
0
50
100
150
200
250
300
350
Lake Maggiore
Lower Lake Lugano
Upper Lake Lugano
Lake Geneva
Upper Lake Constance
Lower Lake Constance
Upper Lake Zurich
Lower Lake Zurich
Lake Zug
Walensee
Rotsee
Lake Neuchâtel
Lake Biel
Lake Murten
Lake Lucerne: Gersauer- and Treibbecken
Lake Lucerne: Urnersee
Lake Lucerne: Alpnachersee
Lake Lucerne: Kreuztrichter and Vitznauerbecken
Hüttwilersee
Greifensee
Lake Lauerz
Lake Hallwil
Inkwilersee
Lake Baldegg
Lake Sarnen
Lago di Vogorno
Mauensee
Lake Sempach
Moossee
Lake Pfäffikon
Lake Thun
Lake Brienz
Soppensee
Amsoldingersee
Türlersee
Lac de la Gruyère
Lake Lungern
Lake Aegeri
Klöntalersee
Sihlsee
Wägitalersee
Lago di Poschiavo
Lac de Joux
Lac Noir
Lac de l'Hongrin
Lake Davos
Oeschinensee
Lake St. Moritz
Lake Silvaplana
Lake Sils
Lago Ritom
Lake Cadagno
Lej da Vadret
Daubensee

~~**Figure 6.**~~

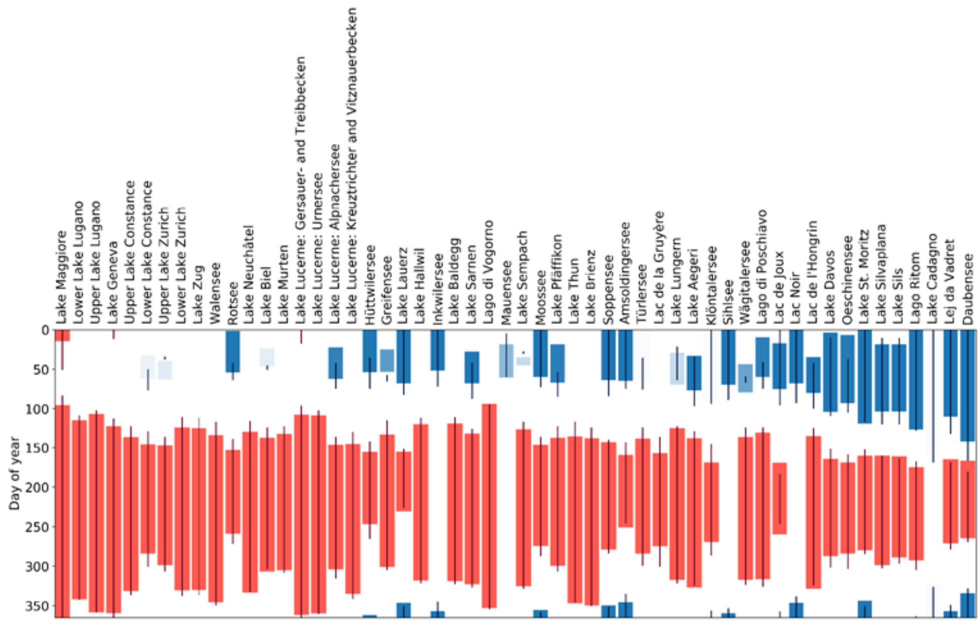

Figure 5. Comparison of timing of stratification and ice cover for the considered lakes. The coloured areas represent the mean periods of summer stratification (red) and ice cover (blue); the vertical lines represent the last year (here, 2017). The transparency for the ice cover indicates the freezing frequency: full transparency means that ice was never modelled, while no transparency means that ice was modelled every winter. Lakes are ordered from left ~~to right based on~~(low elevation~~.~~

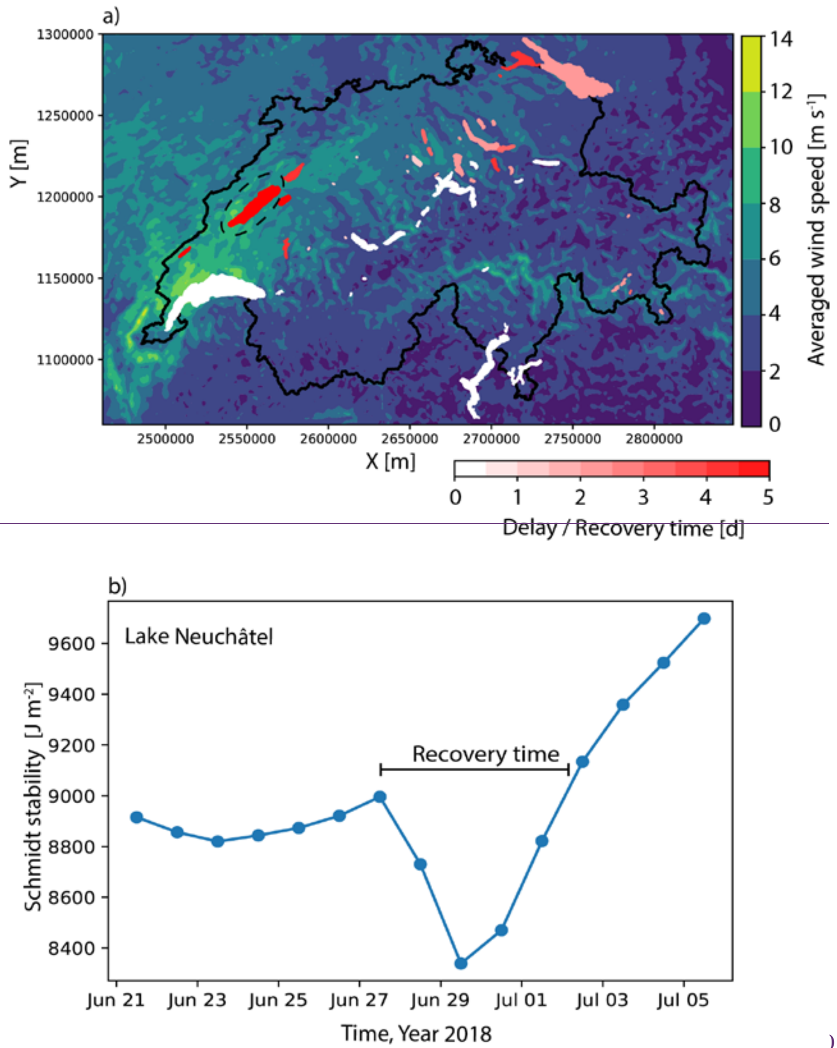

) to right

(high elevation). The time period of data used is indicated in Appendix A.

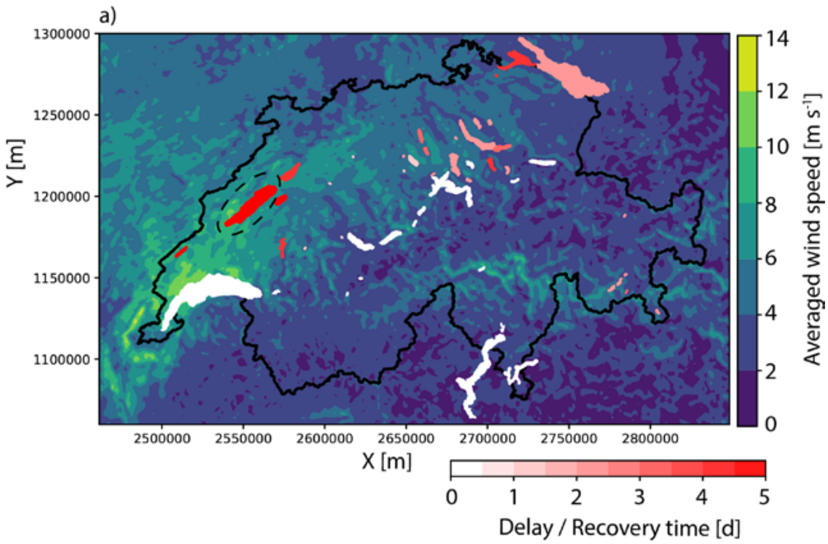
a)
1300000
1250000
1200000
1150000
1100000
Y [m]
2500000
2550000
2600000
2650000
2700000
2750000
2800000
X [m]
14
12
10
8
6
4
2
0
Averaged wind speed [m s-1]
0
1
2
3
4
5
Delay / Recovery time [d]

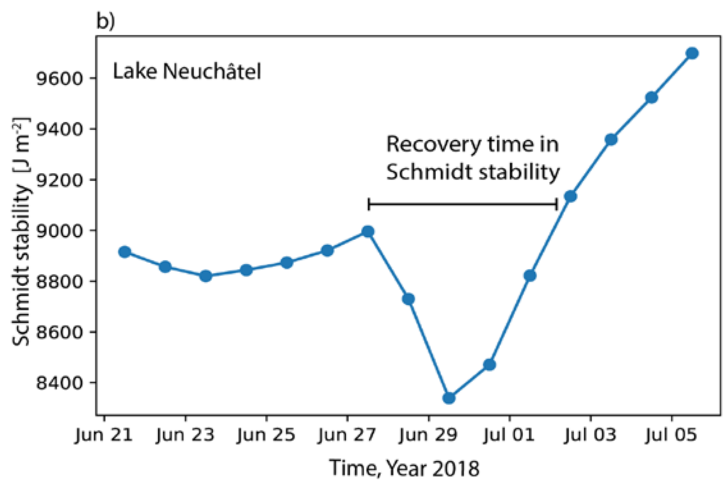
b)
Lake Neuchâtel
Recovery time in
Schmidt stability
9600
9400
9200
9000
8800
8600
8400
Schmidt stability [J m-2]
Jun 21
Jun 23
Jun 25
Jun 27
Jun 29
Jul 01
Jul 03
Jul 05
Time, Year 2018

Figure 76. (a) Mean wind field on June 28th, 2018 (data source: MeteoSwiss, COSMO-1 model, coordinate system CH1903+) and delay in Schmidt stability increase for the modelled lakes: from no delay (white) to a delay of more than 5 days (red). (b) Schmidt stability (daily average) in Lake Neuchâtel during the period of the storm.

Table 1. Input data sources used for the model

Data	Source	Model input
Lake bathymetry	Swisstopo (https://www.swisstopo.admin.ch)	Bathymetry profile
Meteorological forcing	MeteoSwiss (http://meteoswiss.admin.ch)	Air temperature, solar radiation, humidity, wind, cloud cover, precipitation
Hydrological forcing	FOEN (http://hydrodaten.admin.ch)	Inflow discharge, inflow temperature
Secchi depth	Eawag, cantonal monitoring	Light absorption coefficient
CTD profiles	Eawag, cantonal monitoring	Initial conditions, temperature observations for calibration

Table 2. Model parameters. The asterisk (*) indicates the parameters that were calibrated. The geothermal heat flux is based on existing geothermal data for Switzerland: https://www.geocat.ch/geonetwork/srv/eng/md.viewer#/full_view/2d8174b2-8c4a-44ea-b470-cb3f216b90d1.

Parameter	Description and units	Default value
lat	Latitude [°]	Based on lake location
p_air	Air pressure [mbar]	Based on lake elevation
a_seiche*	Ratio of wind energy going into seiche energy [-]	Based on lake size
q_nn	Fractionation coefficient for seiche energy [-]	1.10
f_wind*	Scaling factor for wind speed [-]	1.00
c10	Scaling factor for the wind drag coefficient [-]	1.00
cd	Bottom drag coefficient [-]	0.002
hgeo	Geothermal heat flux [W/m^2]	Based on geothermal map (see table caption)
p_radin*	Scaling factor for the incoming long wave radiation [-]	1.00
p_windf	Scaling factor for the fluxes of sensible and latent heat [-]	1.00
albsw	Albedo of water for short wave radiation [-]	0.09
beta_sol	Fraction of short wave radiation absorbed as heat in the uppermost water layer [-]	0.35
p_albedo*	Scaling factor for snow/ice albedo, thereby affecting melting and under ice warming [-]	1.00
freez_temp	Water freezing temperature [°C]	0.01
snow_temp	Temperature below which precipitation falls as snow [°C]	2.00

Appendix

A. Properties of the modelled lakes

The following table summarizes the main properties of the 54 lakes we model in this work. The full dataset is available as a JSON file. An asterisk after the lake name indicates that this lake was not calibrated due to the lack of observational data. MeteoSwiss = (Swiss) Federal Office of Meteorology and Climatology. FOEN = (Swiss) Federal Office for the Environment. # indicates lakes where secchi disk depth are available. For lakes with clearly defined multi basin such as Lake Lucerne, Lake Zurich, Lake Constance and Lake Lugano, each basin is considered as a separated lake connected to the other basins by inflows/outflows

Lake		Volume [km^3]	Surface [km^2]	Max depth [m]	Retention time [y]	Elevation [m]	Trophic state	Weather station IDs (MeteoSwiss)	Hydrological station IDs (FOEN)	Model timeframe
Lake Aegeri 689574 / 191747	1	0.36	7.3	83	~ 6.8	724	O	AEG, SAG, EIN	-	2012-2018
Lake Baldegg 662239 / 228077	2	0.174	5.2	66	~ 4.2	463	E	MOA	-	2012-2018
Lake Hallwil 658779 / 237484	3	0.285	10.3	48	~ 3.9	449	E	MOA	2416	2012-2018
Lake Biel 578599 / 214194	4	1.12	39.3	74	~ 0.16	429	E#	CRM	2085, 2307, 2446	1993-2018
Upper Lake Constance 749649 / 275225	5	47.6	473	251	~ 4.3	395	M#	ARH, GUT	2473, 2308, 2312	1981-2018
Lower Lake Constance 718479 / 285390	6	0.8	63	45	~ 0.05	395	M	STK, HAI, GUT	-	1981-2018

Inserted Cells
Formatted: Font: 8 pt
Inserted Cells
Formatted: Font: 8 pt
Inserted Cells
Formatted: Font: 8 pt
Formatted: Font: 8 pt
Formatted: Font: 8 pt
Formatted: Font: 8 pt
Formatted: Font: 8 pt
Formatted: Font: 8 pt
Formatted: Font: 8 pt
Formatted: Font: 8 pt
Formatted: Font: 8 pt
Formatted: Font: 8 pt
Formatted: Font: 8 pt
Formatted: Font: 8 pt
Formatted: Font: 8 pt
Formatted: Font: 8 pt
Formatted: Font: 8 pt
Formatted: Font: 8 pt
Formatted: Font: 8 pt
Formatted: Font: 8 pt
Formatted: Font: 8 pt
Formatted: Font: 8 pt
Formatted: Font: 8 pt
Formatted: Font: 8 pt
Formatted: Font: 8 pt
Formatted: Font: 8 pt
Formatted: Font: 8 pt
Formatted: Font: 8 pt
Formatted: Font: 8 pt
Formatted: Font: 8 pt
Formatted: Font: 8 pt
Formatted: Font: 8 pt
Formatted: Font: 8 pt
Formatted: Font: 8 pt
Formatted: Font: 8 pt
Formatted: Font: 8 pt

Lake Brienz 640709 / 175275	7	5.17	29.8	259	~ 2.7	564	O#	INT	2019, 2109	1981-2018
Lake Thun 619899 / 172630	8	6.5	48.3	217	~ 1.9	558	O#	THU, INT	2457, 2469, 2488	1981-2018
Lake Geneva 533600 / 144624	9	89	580	309	~ 11	372	M#	PUY	2009, 2432, 2433, 2486, 2493	1981-2018
Greifensee 693699 / 245032	10	0.15	8.5	32	~ 1.1	435	E	SMA	-	1981-2018
Lac de la Gruyère 573990 / 168654	11	0.22	9.6	75	~ 0.4	677	NA	MAS, GRA	2160, 2412	2011-2018
Klöntalersee 716984 / 209627	12	0.056	3.3	45	~ 0.5	848	O	GLA	-	1981-2018
Lac de Joux 511590 / 165965	13	0.145	8.77	32	0.85	1004	M	CHB, BIE	-	2009-2018
Lago di Vogorno* 709279 / 118833	14	0.1	1.68	204	A	470	O	OTL	2605	1981-2018
Lake Maggiore 694300 / 92576	15	37	212	372	~ 4	193	O	OTL	2068, 2368	1981-2018

Upper Lake Lugano 721139 / 95471	16	4.69	27.5	288	~12.3	271	E	LUG	2321	1981-2018
Lower Lake Lugano 714239 / 86391	17	1.14	20.3	95	~ 1.4	271	M	LUG	2629, 2461	1981-2018
Lake Lungern 655099 / 183325	18	0.065	2	68	~ 0.6	688	NA	GIH	-	2010-2018
Lake Murten 572700 / 198094	19	0.55	22.8	45	~ 1.2	429	M#	NEU	2034	1981-2018
Lake Neuchâtel 554800 / 194974	20	13.8	218	152	~ 8.2	429	M#	NEU	2378, 2369, 2480, 2458, 2447	1981-2018
Lake Pfäffikon 701604 / 245377	21	0.059	3.3	36	~ 2.1	537	M	SMA	-	1981-2018
Lake Sempach 654629 / 221355	22	0.66	14.5	87	~ 16.9	504	M	EGO	2608	2010-2018
Lake Sarnen 658349 / 190767	23	0.239	7.5	51	~ 0.8	469	O	GIH	-	2010-2018
Lake Lucerne: Alpnachersee 667144 / 202267	24	0.1	4.5	35	~ 0.3	434	O	LUZ	2102, 2436	1981-2018

Lake Lucerne: Urnersee 688649 / 200895	25	3.16	22	200	~ 2.0	434	O	ALT	2056, 2276	1981-2018
Lake Lucerne: Gersauer- and Treibbecken 681659 / 203585	26	4.41	30	214	~ 1.6	434	O	GES, ALT	2084, 2481	1981-2018
Lake Lucerne: Kreuztrichter and Vitznauerbecken 672049 / 208875	27	4.35	59	151	~ 0.7	434	O	LUZ	-	1981-2018
Walensee 735739 / 202690	28	2.5	24.2	151	~ 1.4	419	O	QUI, LAC, GLA	2372, 2426	1981-2018
Lake Zug 680049 / 216865	29	3.2	38.3	197	~ 14.7	417	E	CHZ, WAE	2477	1981-2018
Sihlsee 701504 / 222387	30	0.096	11.3	22	~ 0.4	889	O	EIN	2300, 2635	2012-2018
Wägitalersee* 701504 / 222387	31	0.15	4.18	65	~ 1.6	900	O	LAC, EIN	-	2012-2018
Upper Lake Zurich 707159 / 229595	32	0.47	20.3	48	~ 0.69	406	M	WAE	2104	1981-2018

Lower Lake Zurich 687209 / 237715	33	3.36	68.2	136	~ 1.4	406	M#	LAC, SCM, WAE	-	1981-2018
Lago di Poschiavo 804706 / 128871	34	0.12	1.98	85	~ 0.5	962	O	ROB	2078	1981-2018
Lake Sils 776533 / 143922	35	0.137	4.1	71	~ 2.2	1797	O	SIA	-	2014-2018
Lake Silvaplana 780801 / 146926	36	0.14	2.7	77	~ 0.7	1791	O	SIA	-	2014-2018
Lake St. Moritz 784870 / 152099	37	0.02	0.78	44	~ 0.1	1768	O	SAM	2105	1981-2018
Lake Lauerz 688864 / 209546	38	0.0234	3.07	14	~ 0.3	447	M	GES, LUZ	-	1981-2018
Rotsee 666491 / 213558	39	0.00381	0.48	16	~ 0.4	419	E	LUZ	-	1981-2018
Daubensee* 613862 / 140026	40		0.64	50	NA	2207	O	BLA	-	2013-2018
Lej da Vadret* 785308 / 141515	41		0.43	50	NA	2160	O	SIA	-	2014-2018

Lake Davos* 784261 / 188317	42	0.0156	0.59	54	NA	1558	O	DAV	-	1981-2018
Lac de l'Hongrin* 569975 / 141537	43	0.0532	1.6	105	NA	1250	O	CHD	-	2012-2018
Türlersee 680514 / 235858	44	0.00649	0.497	22	~ 2	643	E	WAE	-	1981-2018
Amsoldingersee 610534 / 174906	45	0.00255	0.382	14	NA	641	E#	THU	-	2012-2018
Lac Noir* 587970 / 168280	46	0.00252	0.47	10	NA	1045	M	PLF	-	1989-2018
Moossee 603165 / 207928	47	0.00339	0.31	21	NA	521	E	BER	-	1981-2018
Mauensee 648258 / 224587	48		0.55	9	NA	504	E	EGO	-	2010-2018
Oeschinensee 622116 / 149701	49	0.0402	1.11	56	~ 1.6	1578	O	ABO	-	1983-2018
Soppensee 648765 / 215720	50	0.00286	0.25	27	~ 3.1	596	E	EGO	-	2010-2018

Inkwilersee	51	0.00094	0.102	6	~ 0.1	461	E#	KOP	-	2011-2018
617009 / 227527										
Hüttwilersee	52		0.34	28	NA	434	E	HAI	-	2010-2018
705538 / 274275										
Lake Cadagno	53	0.00242	0.26	21	~ 1.5	1921	E	PIO	-	1981-2018
697683 / 156223										
Lago Ritom*	54	0.048	1.49	69	NA	1850	O	PIO	-	1981-2018
695933 / 155169										

Formatted: Font: 8 pt
Formatted: Font: 8 pt
Formatted: Font: 8 pt
Formatted: Font: 8 pt
Formatted: Font: 8 pt
Formatted: Font: 8 pt
Inserted Cells
Formatted: Font: 8 pt
Formatted: Font: 8 pt
Formatted: Font: 8 pt
Formatted: Font: 8 pt
Formatted: Font: 8 pt
Formatted: Font: 8 pt
Inserted Cells
Formatted: Font: 8 pt
Formatted: Font: 8 pt
Formatted: Font: 8 pt
Formatted: Font: 8 pt
Formatted: Font: 8 pt
Formatted: Font: 8 pt
Formatted: Font: 8 pt
Formatted: Font: 8 pt
Formatted: Font: 8 pt

Meteorological station	Abreviation	Altitude (m.a.s.l)	Coordinates (CH)
Oberägeri	AEG	724	688728 / 220956
Sattel	SAG	790	690999 / 215145
Einsiedeln	EIN	911	699983 / 221068
Mosen	MOA	453	660128 / 232851
Cressier	CRM	430	571163 / 210797
Altenrhein	ARH	398	760382 / 261387
Güttingen	GUT	440	738422 / 273963
Steckborn	STK	397	715871 / 280916
Salen-Reutenen	HAI	719	719099 / 279047
Interlaken	INT	577	633023 / 169092
Thun	THU	570	611201 / 177640
Pully	PUY	456	540819 / 151510
Zürich / Fluntern	SMA	556	685117 / 248066
Marsens	MAS	715	571758 / 167317
Fribourg / Posieux	GRA	651	575184 / 180076
Les Charbonnières	CHB	1045	513821 / 169387
Bière	BIE	684	515888 / 153210
Locarno / Monti	OTL	367	704172 / 114342
Lugano	LUG	273	717874 / 95884
Giswil	GIH	471	657322 / 188976
Neuchâtel	NEU	485	563087 / 205560
Egolzwil	EGO	522	642913 / 225541

Luzern	LUZ	454	665544 / 209850
Altdorf	ALT	438	690180 / 193564
Gersau	GES	521	682510 / 205572
Quinten	QUI	419	734848 / 221278
Laschen / Galgenen	LAC	468	707637 / 226334
Glarus	GLA	517	723756 / 210568
Cham	CHZ	443	677758 / 226878
Wädenswil	WAE	485	693847 / 230744
Schmerikon	SCM	408	713725 / 231533
Plaffeien	PLF	1042	586825 / 177407
Segl-Maria	SIA	1804	778575 / 144977
Blatten, Lötschental	BLA	1538	629564 / 141084
Adelboden	ABO	1322	609350 / 149001
Piotta	PIO	990	695880 / 152265

B. Ice module

The ice and snow module employed is based on the work of Leppäranta (2014, 2010) and Saloranta and Andersen (2007), and includes the following physical processes:

- Air temperature dependent formation and growth of black ice, including the insulating effect of a snow cover.
- Snow layer build-up, including the compression effect due to the weight of fresh snow.
- Buoyancy-driven formation of white ice.
- Short wave irradiance reflection and penetration into the underlying water column.
- Melting of snow, white and black ice due to both the direct heat flux through the atmospheric interface and the absorption of short wave irradiance.

Three layers are used to represent black ice, white ice, and snow. An instant supply of water through cracks in the black ice is assumed to occur in order to form white ice. The water stored in ice and snow is neither withdrawn during ice formation nor added during melting to the water balance. Furthermore, the effect of liquid water pools on top of or between the layers is neglected

Below the freezing point (ice formation)

The ice module is activated as the water temperature in the topmost grid cell T_w (°C) drops below the freezing temperature T_f (°C). T_f can be set to zero for a vertical grid size ≤ 0.5 m, the user can adapt (raise) this value to fit coarser grids. If temperature is below the freezing point, the energy incorporated into the change of state E_f is calculated as

$$E_f = \rho_w c_{pw} z_1 (T_f - T_w) \tag{B1}$$

here ρ_w (1000 kg m^{-3}) is the density of fresh water, c_{pw} the heat capacity of water (4182 J kg^{-1} °C^{-1}) and z_1 the height of the topmost grid cell. E_f and the latent heat of freezing l_h (3.34·10^5 J kg^{-1}) as well as the density of black ice ρ_{ib} (916.2 kg m^{-3}) are used for calculating the initial height of black ice h_{ib} (m) in Eq. B2, thereafter T_w is set equal to T_f

$$h_{ib} = E_f / (l_h \rho_{ib}) \tag{B2}$$

If an ice cover is present and if the atmospheric temperature T_a (°C) is smaller or equal to T_f, the growth of black ice dh_{ib}/dt continues as described in (Saloranta and Andersen, 2007).

$$\frac{dh_{ib}}{dt} = \sqrt{2k_i / (\rho_{ib} * l_h) * (T_f - T_i)} \tag{B3}$$

Here k_i (2.22 W K^{-1} m^{-1}) is the thermal conductivity of ice at 0 °C and T_i (°C) the ice temperature calculated as

$$T_i = \frac{PT_f + T_a}{1 + P} \tag{B4}$$

$$P = \max\left(\frac{k_i h_s}{k_s h_{ib}}, \frac{1}{10 h_{ib}}\right) \tag{B5}$$

There k_s (0.2 W K^{-1} m^{-1}) is the thermal conductivity of snow and h_s (m) the height of the snow layer. When T_a is smaller than the snow temperature (default set to 2 °C) water equivalent precipitation p_r (m hour^{-1}) is turned into fresh snow h_{s_new} (m) as

$$h_{s\_new} = p_r \frac{\rho_w}{\rho_{s0}} \tag{B6}$$

where ρ_{s0} (250 kg m^{-3}) is the initial snow density. The existing snow cover h_s (m) undergoes compression (first terms Eq. B7 and B8) by the new layer as described in Yen (1981), thereafter the new and existing layers are combined in both height and density (second terms of Eqs. B7 and B8).

$$\frac{dh_s}{dt} = -h_s\left(1-\frac{\rho_s}{[\rho_s + d\rho_s]}\right) + h_{s\_new} \tag{B7}$$

$$\frac{d\rho_s}{dt} = \rho_s C_1 w_s e^{-C_2\rho_s} - \left(\rho_s - \frac{\rho_s h_s + \rho_{s0} h_{s\_new}}{h_s + h_{s\_new}}\right) \tag{B8}$$

here ρ_s (kg m^{-3}) is the snow layer density kept within $\rho_{s0} < \rho_s < \rho_{sm}$ with the maximum snow density set to 450 kg m^{-3}, C_1 (5.8 m^{-1} hour^{-1}) and C_2 (0.021 m^3 kg^{-1}) are snow compression constants, and w_s (m) is the total weight above the layer under compression expressed in water equivalent height.

If the snow mass m_s (kg m^{-2}) becomes heavier than the upward acting buoyancy force B_i (kg m^{-2}), white ice with height h_{iw} (m) and density ρ_{iw} (875 kg m^{-3} Saloranta, 2000) is formed between the snow and the black ice layers to achieve equilibrium between B_i and m_s.

$$B_i = h_{ib}\left(\rho_w - \rho_{ib}\right) + h_{iw}\left(\rho_w - \rho_{iw}\right) \tag{B9}$$

$$\frac{dh_{iw}}{dt} = \frac{m_s - B_i}{\rho_s} \tag{B10}$$

In this model, we assume continuous supply of water through cracks in the black ice to form white ice. The formation of white ice takes place instantaneously each time step and we do not consider the influence of pools under the snow for melting or short wave irradiance penetration.

Above the freezing point (melting)

If an ice cover is present and if $T_a > T_f$ melting starts. Each layer melts from above through the atmospheric interface and by penetrating short wave radiation

$$\frac{dh_{x\_upper}}{dt} = -\frac{H_{x\_y}}{(l_h + l_e)\rho_x} \tag{B11}$$

where H_{x_y} (W m^{-2}) is the layer-dependent heat flux (in the following, $_x$ represents $_s$, $_{iw}$ or $_{ib}$). The model supports melting through both sublimation (solid to gas) and non-sublimation (solid to liquid) with the inclusion/exclusion of the latent heat of evaporation l_e (J kg^{-1}). Non-sublimation melting is default with l_e set to zero, for sublimation melting the user can set l_e to 2265 kJ kg^{-1}. For the uppermost layer ($_y$ = $_{top}$, Eq. B12) the heat flux includes layer dependent uptake of short wave radiation H_{s_x}, long wave absorption H_a or layer dependent emission H_{w_x} as well as sensible H_k and latent H_v heat. If the layer is not in direct contact with the atmosphere, only H_s is used for melting from above ($_y$ = $_{under}$, Eq. B13).

$$H_{x\_top} = H_{s\_x} + H_a + H_{w\_x} + H_k + H_v \quad \text{(B12)}$$

$$H_{x\_under} = H_{s\_x} \quad \text{(B13)}$$

Here we follow Leppäranta (2014, 2010) for determining the heat flux terms in Eq. B12. The transmittance of short wave irradiance through each layer depends on each layers thickness h_x as well as on the layer specific bulk attenuation coefficient λ_x (m^{-1}; default λ_s = 24, λ_{iw} = 3 and λ_{ib} = 2; Leppäranta, 2014).

$$H_{s\_s} = I_s A_p \left(1 - A_x\right)\left(1 - e^{\left(-\lambda_s h_s\right)}\right) \quad \text{(B14)}$$

$$H_{s\_iw} = I_s A_p \left(1 - A_x\right)\left(e^{\left(-\lambda_s h_s\right)} - e^{\left(-\lambda_s h_s - \lambda_{iw} h_{iw}\right)}\right) \quad \text{(B15)}$$

$$H_{s\_ib} = I_s A_p \left(1 - A_x\right)\left(e^{\left(-\lambda_s h_s - \lambda_{iw} h_{iw}\right)} - e^{\left(-\lambda_s h_s - \lambda_{iw} h_{iw} - \lambda_{ib} h_{ib}\right)}\right) \quad \text{(B16)}$$

$$H_{s\_w} = I_s A_p \left(1 - A_x\right)\left(1 - e^{\left(-\lambda_s h_s - \lambda_{iw} h_{iw} - \lambda_{ib} h_{ib}\right)}\right) \quad \text{(B17)}$$

There H_{s_w} is the radiation penetrating through the ice cover to the water below and I_s (W m^{-2}) the incoming short wave irradiance. We introduce the albedo parameter A_p which tunes short wave irradiance in order to match observed water temperatures, thus adjusting the melting and indirectly the duration of the ice cover. Furthermore, depending on which layer is in contact with the atmosphere we use a layer dependent constant albedo A_x (default A_s = 0.7, A_{iw} = 0.4 and A_{ib} = 0.3; Leppäranta, 2014).

$$A_x \begin{cases} A_s, h_s > 0 \\ A_{iw}, h_s = 0 \,\&\, h_{iw} > 0 \\ A_{ib}, h_s + h_{iw} = 0 \end{cases} \quad \text{(B18)}$$

Calculating H_a requires the long wave emission parameters k_a = 0.68, k_b = 0.036 (mbar^{-1}) and k_c = 0.18 (Leppäranta, 2010), atmospheric water vapour pressure e_a (mbar), cloud cover C and Stefan Boltzmann's constant σ (5.67*10^{-8} W m^{-2} K^{-4}). For Eqs. B19 and B20 the temperature T_x is given in Kelvin. H_{w_x} is layer dependent for the emissivity E_x with E_{iw} = E_{ib} = 0.97 and $E_s(\rho_s)$ from 0.8 at ρ_s = 250 kg m^{-3} to E_s = 0.9 for ρ_s = 450 kg m^{-3}. Calculating H_k and H_v requires the atmospheric density $\rho_{a\,=}$

1.2 kg m^{-3}, the heat capacity of air c_{pa} = 1005 J kg^{-1} K^{-1}, the wind speed at 10 m height w_{10}, the convective (b_c) and latent (b_l) bulk exchange coefficients both set to 0.0015 (Leppäranta, 2010; Gill, 1982), as well as the specific humidity both measured q_a (mbar) and at saturation q_0. There $q_a = 0.622e_a/p_a$ where p_a is the air pressure and $q_0 = 0.622*6.11/p_a$ at T_a= 0 °C (Leppäranta, 2014).

$$H_a = \left(k_a + k_b\sqrt{e_a}\left[1 + k_c C^2\right]\right)\sigma T_a^4 \quad \text{(B19)}$$

$$H_{w\_x} = E_x \sigma T_f{}^4 \quad \text{(B20)}$$

$$H_k = \rho_a c_{pa} b_c \left(T_a - T_f\right) w_{10} \quad \text{(B21)}$$

$$H_v = \rho_a l_h b_l \left(q_a - q_0\right) w_{10} \quad \text{(B22)}$$

As H_{s_w} warms the water under the ice, melting takes place from underneath with the energy H_{bottom} (W m^{-2}).

$$H_{bottom} = \left(T_w - T_f\right) c_{pw} \rho_w z_1 \quad \text{(B23)}$$

After obtaining H_{bottom} the temperature of the first cell is set to T_f and the decrease of ice cover from below becomes

$$\frac{dh_{x\_lower}}{dt} = -\frac{H_{bottom}}{l_m \rho_x} \quad \text{(B24)}$$

Eq. B24 is only applied to h_{ib} and h_{iw}. In principle, h_s melts completely from above using Eq. B11 before h_{ib} and h_{iw} reach zero, however, if no ice is present, h_s is set to zero. By combining Eqs. B11 and B24 the total melting of each ice layer is calculated as

$$\frac{dh_x}{dt} = \frac{dh_{x\_lower}}{dt} + \frac{dh_{x\_upper}}{dt} \quad \text{(B25)}$$

When $h_x < 0$ due to melting the surplus energy is used for melting neighbouring layers according to the following procedure: if the melting is initiated from above the surplus energy is used to melt the layer directly underneath; if the melting is caused by the water below the layer directly above receives the surplus melting energy; if $h_{ib} <= h_{iw} <= 0$ the water in the topmost grid cell is heated with the remaining energy.

Ice model performance

To test the ice module, Simstrat was calibrated in Sihlsee with PEST using monthly resolved vertical temperature profiles (2006 to 2008, RMSE 1.2 °C) for four parameters including the new p_albedo parameter for scaling snow/ice albedo. Modelled and monthly measured total ice cover from 2012 to 2018 is shown in Fig. B1 (RMSE 0.078 m). The modelled thickness agrees well with measurements during years with an extensive ice covered period (2013, 2014 and 2017, max height > 5 cm). The model performance is not ideal for years with short temporal ice duration and thin ice thickness (2016 and 2018, max height < 5 cm). During these years, the quality of the forcing dataset becomes crucial. In the case of Sihlsee, the timing and duration of snowfall prolongs the duration of the ice-covered period. We use the meteorological station at Samedan (SAM) located four kilometres from the lake in a region with rapid topographical change. This in combination with monthly ice thickness measurements result in the divergence during 2016 and 2018.

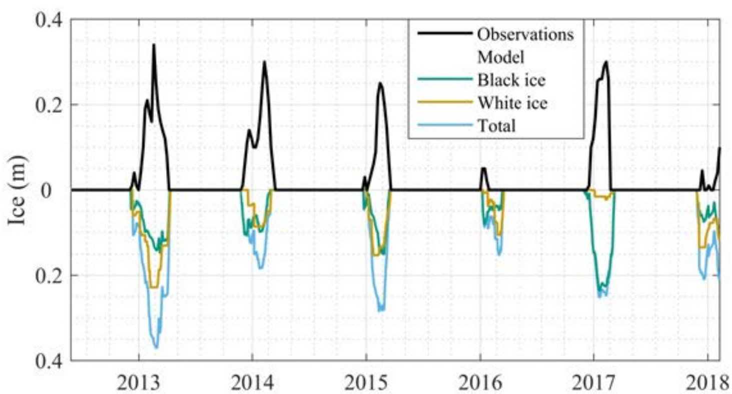

Figure B1. Ice model performance in Sihlsee (2012 to 2018) showing modelled white ice (orange), black ice (green) and total ice cover (white- and black ice combined, in blue) against measurements (black).

C. Estimation of clear-sky solar radiation

The algorithm below is based on the equations from the Lake HeatFluxAnalyzer (see http://heatfluxanalyzer.gleon.org/), following the methods of Meyers and Dale (1983).

Declination of the sun [rad]: $\delta = \sin^{-1}(-0.39779 \cos \frac{2\pi \mathrm{DOY_s}}{365.24})$, where DOY_s is the day of year after the winter solstice (December 21st).

Cosine of the solar zenith angle [-]: $\cos Z = \max(\sin \varphi \sin \delta + \cos \varphi \cos \delta \cos \frac{\pi(\mathrm{H}-12.5)}{12}, 0)$, where φ is the latitude in radians and H is the hour of the day, assuming the solar noon is at 12h30.

Air mass thickness coefficient [-]: $m = 35 \cos Z \,(1244 \cos^2 Z + 1)^{-0.5}$

Dew point temperature [°C]: $T_d = 243.5 \log \frac{p_w}{6.112} / (17.67 - \log \frac{p_w}{6.112}) + 33.8$, where p_w[mbar] is the water vapour pressure.

Precipitable water vapour [cm]: $w_p = e^{0.1133 - \log(G+1) + 0.0393(1.8\, T_d + 32)}$, where G is an empirical constant dependent on latitude and day of year (see tables from Smith, 1966).

Attenuation coefficient for water vapour [-]: $\lambda_w = 1 - 0.077\, (w_p m)^{0.3}$

Attenuation coefficient for aerosols [-]: $\lambda_a = 0.935^m$

Attenuation coefficient for Rayleigh scattering and permanent gases [-]: $\lambda_{Rg} = 1.021 - 0.084(m\,(0.000949 p_a + 0.051))^{0.5}$, where p_a [mbar] is the air pressure.

Effective solar constant [W m^{-2}]: $I_{\mathrm{eff}} = 1353(1 + 0.034 \cos \frac{2\pi \mathrm{DOY}}{365.24})$, where DOY is the day of year.

Clear-sky solar radiation [W m^{-2}]: $H_{\mathrm{cs}} = I_{\mathrm{eff}} \cdot \cos Z \cdot \lambda_w \, \lambda_a \, \lambda_{Rg}$